Green Synthesis of Zinc Oxide with Silicon Oxide Nanocomposite Using *Ajuga Integrifolia* Leaf Extract and its Antibacterial and Photocatalytic Activity

Mengistu Tesfaye Arficho

A Thesis Submitted to the Department of Applied Chemistry

School of Applied Natural Science

Presented in Partial Fulfillment of the Requirements for the Degree of

Master of Science in Applied Chemistry (Industrial chemistry)

Office of Graduate Studies

Adama Science and Technology University

September, 2023

Adama, Ethiopia

Green Synthesis of Zinc Oxide with Silicon Oxide Nanocomposite Using *Ajuga Integrifolia* Leaf Extract and its Antibacterial and Photocatalytic Activity

Mengistu Tesfaye Arficho

Advisor: Aschalew Tadesse (PhD.)
Co-advisor: Buzuayehu Abebe (PhD.)

A Thesis Submitted to the Department of Applied Chemistry
School of Applied Natural Science

In Partial Fulfillment of the Requirements for the Degree of Master of Science in Applied Chemistry (Industrial Chemistry)

Office of Graduate Studies
Adama Science and Technology University

September, 2023
Adama, Ethiopia

Declaration

I hereby declare that this Master Thesis entitled "**Green Synthesis of Zinc Oxide with Silicon Oxide Nanocomposite Using *Ajuga integrifolia* Leaf Extract and its Antimicrobial and Photocatalytic Activity"** is my own work and has not been submitted to any university for a similar purpose. The reference used in this Thesis is duly recognized by proper citation.

______________________	______________________	______________
Name of the Student	Signature	Date

Recommendation

We, the advisor(s) of this Thesis, hereby certify that we have advised the student while developing the Thesis and read the draft of the Thesis entitled "**Green Synthesis of Zinc Oxide with Silicon Oxide Nanocomposite Using *Ajuga Integrifolia* Leaf Extract and its Antibacterial and Photocatalytic Activity**" prepared under our guidance by Mengistu Tesfaye Arficho. Therefore, we recommend the submission of the Thesis to the department for future review and evaluation.

______________________	______________________	________________
Major Advisor	Signature	Date
______________________	______________________	________________
Co-advisor Signature	Signature	Date

Approval Page

We hereby certify that the recommendation and suggestion given by the Thesis review committee are appropriately incorporated into the final thesis entitled "**Green Synthesis of Zinc Oxide with Silicon Oxide Nanocomposite Using *Ajuga integrifolia* Leaf Extract and its Antibacterial and Photocatalytic Activity**" by Mengistu Tesfaye Arficho.

Aschalew Tadesse (PhD)		02/10/2023
Major Advisor	Signature	Date
Birhanu Abebe (PhD)		02/10/2023
Co-advisor	Signature	Date

We, the undersigned, members of the Board of Reviewers of the open defense by Mengistu Tesfaye Arficho have read and evaluated the thesis entitled "**Green Synthesis of Zinc Oxide with Silicon Oxide Nanocomposite Using *Ajuga integrifolia* Leaf Extract and its Antibacterial and Photocatalytic Activity**" and assessed the understanding of the candidate about the proposed research. This is, therefore, to certify that the thesis is accepted and we recommend the implementation of the Thesis.

Dr. Defaru Negera Duke		2/10/2023
Chairperson	Signature	Date
Gemechu Deressa (PhD)		02/10/2023
Internal examiner	Signature	Date
Amare Ayalew (PhD)		02/10/2023
External examiner	Signature	Date

Finally, approval and acceptance of the thesis are contingent upon the submission of its final copy to the Office of Postgraduate Studies (OPGS) through the Department Graduate Council (DGC) and School Graduate Committee (SGC).

Dr. Defaru Negera		2/10/2023
Department Head	Signature	Date
		27/11/2023
School Dean	Signature	Date
Office of Postgraduate Studies, Dean	Signature	Date

ACKNOWLEDGEMENT

I am grateful to the almighty of God for the good health and well-being that were necessary to complete this work. To Him alone, I give all the glory. Then I would like to give my honorable thanks to Adama Science and Technology University as a whole and also to SoANS and the Department of applied chemistry in particular for giving me this chance. And foremost, the completion of this Thesis, work will not be possible without the excellent guidance of my advisor Aschalew Tadesse (PhD.). I acknowledge all his encouragement, constructive support, expert advice, technical assistance, and valuable time given to me with deep gratitude and appreciation.

Moreover, my heart felt appreciation goes to my co-advisor Buzuayehu Abebe (PhD.) for his constructive feedback suggestions that have extremely valuable. I appreciate his tremendous encouragement, understanding, and arranging of thesis facilities.

Most importantly, I would like to extend my most profound gratitude to my wife Tsegenash Birhanu for her sincere love, help, and encouragement during my entire study period.

I sincerely acknowledge my honorable family member Mr. Tegesse Shaimalo for his PC support.

Finally, I would like to express my sincere gratitude to Mr. Wolde Shanko, Mr. Habtamu Kifle, Sister Tizita Birhanu, and Mr. Tsedeke Tsegaye for providing financial support, and encouragement.

Table of Contents

Contents page

List of Figures

List of Tables

List of Abbreviations

AOP	Advanced Oxidation Processes
A. *Integrifolia*	*Ajuga integrifolia*
E. Coli	*Escherichia coli*
FTIR	Fourier Transform Infrared
IFT	Inter Facial Tension
JCPDS	Joint committee on powder diffraction standards
MB	Methylene Blue
NPs	Nanoparticles
NC	Nanocomposite
P. *Aeruginosa*	*Pseudomonas Aeruginosa*
S. *Aureus*	*Staphylococcus Aureus*
SEM	Scanning Electron Microscopy
S. PY	*Streptococcus Pyogenesis*
UV-Vis	Ultraviolet Visible Spectroscopy
XRD	X-Ray Diffraction

Abstract

In material science one of the important materials which got attention of researcher is zinc oxide nanoparticles (ZnO NPs) as its property makes usable for different applications such as electronics, catalysis and antimicrobial agent. Making nanocomposite of ZnO with suitable materials improve the property of materials like stability, multiplied surface vicinity, and stepped-forward dispersion of the nanoparticles and silicon oxide (SiO_2) is among the suitable materials. SiO_2 is an amorphous, white, non-toxic powder and the surface of SiO_2 has high activity, good adsorption capacity, and excellent applications as a carrier material, solving the issue of particle agglomeration. In this study, Ajuga integrifolia (A. integrifolia) leaf extract was used for green synthesize of zinc oxide nanoparticle (ZnO NPs), silicon oxide nanoparticles (SiO_2 NPs), and zinc oxide/silicon oxide (ZnO/SiO_2) nanocomposite (NC). The synthesized nanomaterials were characterized by Ultraviolet-Visible (UV-Vis) spectrophotometer, Fourier Transform Infrared (FTIR) spectrometer, X-Ray Diffraction (XRD), and Scanning Electron Microscope (SEM). Each synthesized materials show their representative peaks matched with their joint committee on powder Diffraction Standards (JCPDS) card no.= 036-1451 for ZnO NPs, 043-569 for SiO_2 NPs, and 045-1374 and 036-1451 for ZnO/SiO_2 NCs in X-ray diffraction analysis. The crystalline size calculated based on XRD data was 20.886 nm for ZnO NPs and 8.1737 nm for ZnO/SiO_2 NCs. Ultraviolet-Visible (UV-Vis) spectrophotometer analysis shown characteristic absorption maxima for ZnO NPs at 351.4 nm while that for ZnO/SiO_2 NC shifted to 356 nm. The SEM analysis revealed spherical shape for green synthesized ZnO NPs and ZnO/SiO_2 NCs. The antibacterial activity of synthesized nanomaterials was tested against Gram-positive and Gram-negative. ZnO/SiO_2 NC illustrated high antibacterial activity compared to ZnO NPs. The photocatalytic activity of ZnO/SiO_2 NC was evaluated by the degradation of methylene blue (MB) dye under open visible light irradiation; the results indicated 97.5% degradation at optimum condition. The degradation efficiency of MB dye by using green synthesized ZnO NP was about 95%.

Keywords: *ZnO/SiO_2NC, green synthesis, Ajuga integrifolia, Antibacterial activity, photocatalytic degradation.*

CHAPTER ONE

1 Introduction

1.1. Background

Zinc oxide (ZnO) is a versatile material with numerous applications in various fields such as electronics, optoelectronics, catalysis, and antibacterial agents. However, the conventional methods for the synthesis of ZnO nanoparticles often involve the use of toxic chemicals and high-energy processes, which can be detrimental to the environment and human health. To address these concerns, green synthesis approaches have gained increasing attention in recent years, which involve the use of natural extracts as reducing agents and stabilizers (Jamdagni et al., 2016).

Zinc oxide is an inorganic compound with the formula ZnO. It usually appears as a white powder, nearly insoluble in water. Zinc oxide, with its unique physical and chemical properties, such as high chemical stability, high electrochemical coupling coefficient, a broad range of radiation absorption, and high photostability, is a multifunctional material. A broad energy band (3.37 eV), high bond energy (60 meV), and high thermal and mechanical stability at room temperature make it attractive for potential use in electronics, optoelectronics, and laser technology (Rl et al., 2019). The piezo- and pyroelectric properties of ZnO mean that it can be used as a sensor, converter, energy generator, and photocatalyst in hydrogen production. They also possess antibacterial qualities that protect against tiny organisms and infections that are present in food (Muhammad et al., 2021). ZnO-NPs have been used in various food-packaging coatings to keep up nourishment hues, prevent food deterioration, and improve packaging material properties, including mechanical quality, hindrance properties, and stability (Al-Tayyar et al., 2020). Above mentioned reviewers, ZnO NPs synthesized in different methods for different purposes. But the ZnO NPs synthesized methods and the reagents are difficult to use and expensive meaning not environmentally easily available. As a result, it is necessary to increase the efficiency of ZnO NPs by utilizing an eco-friendly, widely accessible, cost-effective, non-toxic, and green synthetic technique. Therefore, by making the composite of ZnO with SiO_2 NPs improved the efficiency of ZnO NPs on antibacterial and photodegradation of environmental pollutants. The photocatalytic activity of ZnO/SiO_2 NC was evaluated by the degradation of methylene blue (MB) dye under visible light irradiation; the results indicated 97.5% degradation efficiency of MB by using pH 6, 75 mg of catalyst, 25 ppm concentration of dye, and 30 minute UV light irradiation. The degradation efficiency of MB dye by using ZnO NP was obtained 95%.

Ajuga Integrifolia plant species that is widely distributed in various regions of the country and is known for its medicinal value. The plant includes various bioactive compounds which include flavonoids, phenols, and terpenoids, that have been shown to own antioxidant, anti-inflammatory, and antimicrobial activities (Yang et al., 2020). ZnO NPs have been manufactured by numerous researchers utilizing various plant extracts and materials, but these materials are not sufficiently and efficiently applied in rural community (Carrouel et al., 2020).

Silicon oxide (SiO_2) is some other broadly used in various fields inclusive of electronics, coatings, and biomedical applications (Shafiei et al., 2021). The addition of SiO_2 to ZnO can shape a nanocomposite that lead to advanced uses such as: inclusive of greater stability, multiplied surface vicinity, and stepped-forward dispersion of the nanoparticles. Moreover, the aggregation of ZnO and SiO_2 has been shown advanced antibacterial properties in comparison to ZnO NPs. SiO_2 is an amorphous, white, non-toxic powder. The surface of SiO_2 has high activity, good adsorption capacity, and excellent applications as a carrier material, solving the issue of particle agglomeration, and increasing the service life of the antibacterial agent (Carrouel et al., 2020).

In this study zinc oxide and silicon oxide (ZnO/SiO_2) nanocomposite with improved efficiency, size, and other properties, were synthesized following green method using *Ajuga integrifolia* plant extract. The green synthesized ZnO/SiO_2 NCs was used in investigating antibacterial activity and methylene blue dye photodegradation activity.

1.2. Statement of The Problem

There are some basic problems that motivate to conduct of green synthesis of ZnO/SiO_2 nanocomposites using *Ajuga integrifolia* leaf extract and its application for antibacterial and photocatalytic activity. The first one is an increment of bacterial infectious diseases from day to day and increase in bacterial resistance to traditionally used antimicrobials; it has become more difficult for communities to empirically select an appropriate antimicrobial agent (Farrukh, 2016). Different antibacterial drugs are produced from different species of bacteria and also from some plants. However, some antibacterial drugs are very expensive and some are toxic to humans and environments (Kokabi et al., 2017). There is a need for developing the simplest methods of synthesizing low-cost and nontoxic drugs for our communities to save and sound their survival and health from various ailments. In this research, the ZnO/ SiO_2 nanocomposite was synthesized by utilization of bioactive compounds present in *Ajuga integrifolia* leaf extract.

1.3. Objectives

1.3.1. General Objective

The main objective of this research is to synthesize ZnO/SiO_2 nanocomposite using Ajuga *integrifolia* medicinal plant leaf extract and investigate its antimicrobial, and photocatalytic activity.

1.3.2. Specific Objectives

- To synthesize ZnO NPs from zinc acetate salt by utilization of *Ajuga integrifolia* leaf extract.
- To synthesize SiO_2 NPs using Ajuga *integrifolia* leaf extract and TEOS as precursor.
- To synthesize ZnO/SiO_2 NCs from zinc acetate salt and Tetraethylorthosilicate by utilization of *Ajuga integrifolia* leaf extract.
- To characterize the synthesized nanomaterials using XRD, FTIR spectrometer, SEM, and Uv Vis spectrophotometer
- To evaluate the performance of the synthesized ZnO/SiO_2 NCs for photocatalytic degradation of methylene blue and antibacterial activity against bacteria species.

1.4. Significance of The Study

This study gives information to the scientific community about green synthesis and helps to use ZnO/SiO_2 NCs synthesized using a medicinal plant as antimicrobial agents at a low cost. It provided scientific knowledge on how to produce the NCs which are nontoxic and their activity in different applications such as antibacterial, and photocatalytic degradation of environmental pollutant.

1.5. Scope of The Study

This research work limited to the green synthesis of ZnO/SiO_2 NCs using Ajuga *integrifolia* medicinal plant leaf extract, their characterization of the synthesized NCs using UV-Vis spectrophotometer, XRD, FTIR spectrometer, and SEM techniques, investigating its photocatalytic degradation efficiency for representative dye methylene blue and evaluating their antibacterial efficacy against bacterial strains *Escherichia coli* and *Staphylococcus aureus* by using disc diffusion methods.

CHAPTER TWO

2. Literature Review

2.1 Nanotechnology

Nanotechnology has been defined as a technology that mainly consists of the process of separation, consolidation, and deformation of materials by one atom or molecule. The field of nanotechnology is one of the most active areas of research in modern materials science (Narendra Kumar et al., 2019).

Nanotechnology is the science and technology of small things, in particular, things that are less than 100 nm in size. It deals with the production and usage of material with nanoscale dimensions. The nanoscale dimension provides nanoparticles with a large surface area to volume ratio and thus very specific properties. Nanostructured objects with nanometer-scale features are not new and they were not first created by man. There are many examples of nanostructures in nature in the way that plants and animals have evolved. Similarly, there are many natural nanoscale materials, such as catalysts, porous materials, certain minerals, soot particles, etc., that have unique properties, particularly because of the nanoscale features. In the past decade, innovations in our understanding of nanotechnology have enabled us to begin to understand and control these structures and properties in order to make new functional materials and devices (Pelgrift & Friedman, 2013).

2.2. Nanoparticles (NPs)

Nanoparticles are particles in the nanoscale size between 1nm and 100 nm with a surrounding interfacial layer. They are very small particles with improved thermal conductivity, catalytic reactivity, nonlinear optical performance, and chemical stability due to their larger surface area-to-volume ratio (Fabiana Meijon Fadul, 2019). Nanoparticles are of interest because of their high reactivity due to the large open area-to-mass ratio. It has been noted that nanomaterials display different properties at nanometer sizes compared to the properties of the same materials in bulk conditions. The considered properties of nanoparticles are size and anatomy (branch of morphology) in the range of nanoscale. Metal oxide nanoparticles have wide applications, primarily in the technology field, including their use as a semiconductor, electroluminescent, or thermoelectric material, and they are also used in biomedical applications such as drug delivery systems for treatment and diagnosis and in environmental decontamination applications (Zharov et al., 2005).

Nanoparticles also have been integrated into various industrial, health, food, feed, space, chemical, and cosmetics industries of consumers which calls for a green and environment-friendly approach to their synthesis. Among various metal oxide and metal nanoparticles that exist, zinc oxide and silicon oxide nanoparticles have attracted the attention of many researchers owing to their various applications in the electronics, communications, sensors, cosmetics, environmental protection, and biological and medicinal industries (Sportelli et al., 2022).

2.2.1. Zinc Oxide Nanoparticles

Zinc oxide (ZnO) is an n-type semiconductor with a conductivity of about 10^{-7} -10^{-3} S/cm and has a relatively large binding energy of 60 meV, but it has a high band gap energy of about 3.37 eV. The high band gap energy (3.0–3.9 eV) limits the use of ZnO for wider applications because it is only active in the UV light area (Naseer et al., 2020). Due to these properties, they show various semiconducting properties such as high catalytic activity, wound healing, anti-inflammatory, and ultraviolet filtering properties and are extensively used in various cosmetics such as sunscreens. These nanoparticles are used in various biomedical applications too such as antifungal, antibacterial, drug delivery, anti-diabetic, and anticancer (Galedari & Rahmani, 2016). ZnO NPs are environment-friendly as they are compatible with organisms; which makes them suitable for the treatment of water and wastewater. It can absorb a wider range of solar spectra and more light quanta than several semiconducting metal oxides (Fatimah et al., 2021).

2.2.2. Silicon Oxide Nanoparticles

Silicon dioxide (SiO_2) is a compound of Silicon and Oxygen, commonly called silica and the elements are linked by a covalent bond. It is one of the components of the sand and can be found naturally in Quartz. It is usually white or colorless and is not soluble in water or ethanol. By associating with minerals, it forms the silicate family. Silicon dioxide (SiO_2) has several industrial applications such as an additive in the food industry. Its function is to act as an anti-binder, anti-foaming agent, viscosity controller, desiccant, beverage clarifier, and as excipient of medications and vitamins. Due to its insolubility in water, silica has little biological availability and is not considered a source of silicon. Silicon found in other more soluble forms contributes to the formation and maintenance of bones and cartilage (Saravanan, 2020).

Silicon dioxide is a solid and colorless crystalline substance. Silicon dioxide does not react with water and is resistant to acids. The molecular formula of the substance is SiO_2. Silicon oxide, a member of the group of acidic glass-forming oxides, interacts with increasing temperature with alkalis and basic oxides, soluble in hydrofluoric acid, tends to form a supersonic fusion, that is, glass is an excellent dielectric (P. Sharma et al., 2021). The main properties are stated below:

- SiO_2 Nanoparticles is transparent and its density is 2634 kg/m^3.
- The molar mass of SiO_2 is 60.0843 g/mol.
- The melting point is 1986 K, whereas the boiling point is 2503 K.
- Its crystal structure is Quartz, cristobalite or tridymite.

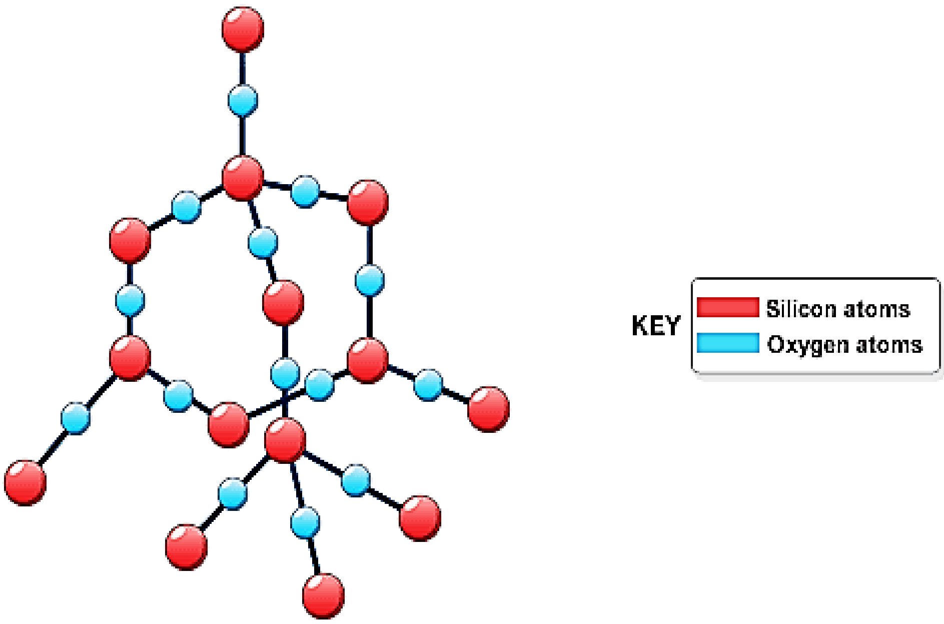

FIGURE 1: Crystal Structure of SiO_2 NP (P. Sharma et al., 2021)

The most durable and inexhaustible element on Earth is silicon, a metalloid that is mostly present as silicate and silica (SiO_2). Plastics were infused with silicon dioxide nanoparticles (SiO_2-NPs) to improve their mechanical properties and thermal stability (Al-Tayyar et al., 2020). SiO_2 nanoparticles were used in a variety of medical procedures, including cancer treatment and drug administration. SiO_2 is a very important matrix as well, possessing excellent compatibility with other materials, huge surface areas, great chemical resistance, and nontoxicity (Javan et al., 2020).

2.3 Synthesis of Zinc Oxide Nanoparticles

Several techniques have been used to create ZnO nanoparticles. ZnO NPs can be obtained using chemical, physical or biological methods (Faisal, Jan, Shah, Shah, Khan, Akbar, Rizwan, Jan, Wajidullah, et al., 2021).

2.3.1 Chemical Methods

The methods included precipitation, microemulsion, chemical reduction, sol-gel, and hydrothermal techniques, which may lead to high energy consumption when high pressure or temperature conditions are required in the process. Developing nanoparticles has made use of plant components such as fruits, seeds, stems, leaves, and roots (Ruhul & Bhuiyan, 2021). The concentration of the chemicals employed in the process can also have a considerable impact on the size and form of the particles, which is an important element to take into account when considering chemical synthesis. It is known that it is possible to obtain particles from a few nanometers (5–10 nm) up to micrometric size using the same process but different concentrations and ratios of chemicals (Sampson, 2019).

2.3.2 Physical Methods

ZnO NPs can be synthesized via physical techniques by vapor deposition, plasma, and ultrasonic irradiation (Bandeira et al., 2020). Nonetheless, these techniques usually require a high amount of energy and robust equipment, which increases the cost of the products.

2.3.3. Green Synthesis Methods of ZnO NPs

The interest in synthesizing ZnO NPs via green methods has increased considerably in the last 10 years. The development of this new approach and the significant interest in it are mainly related to the absence of toxic chemicals or a high amount of energy applied to the green synthesis, which makes the process more cost-effective and eco-friendly (Bandeira et al, 2020).

Zinc oxide nanoparticles can be prepared from different microorganisms (yeast, fungi, bacteria, etc.) and plant tissues (leaves, fruit, latex, peel, flower, root, stem, etc.). These biological methods have become more commonly known as green synthesis. It was also given this term because it is in agreement with the twelve principles of green chemistry.

2.4 Synthesis of SiO_2 Nanoparticles

Plenty of procedures were used to synthesize silica nanoparticles, including processing microemulsion, chemical vapor deposition, combustion synthesis, hydrothermal techniques, plasma synthesis, sol-gel processing, etc. Regardless of the synthesis process, controlling particle shape, surface reactivity, and size was the key goal. A sol-gel procedure that involves the metal alkoxide simultaneous hydrolysis and condensation reaction is the most widely. As reported by Zhang *et al*. demonstrated silica-based nanofluid stability, size and thermal conductivity, and economic silica production from RH source; moreover, anionic surfactant, SDS, moderate role in stabilization has been observed through electrostatic stabilization.

2.5. Nanocomposite (NCs)

A composite material consists of a combination of two materials of different natures completing and allowing us to obtain a material of which the set of performance characteristics is greater than that of the components taken separately (Kumud & Sanju, 2018). A Nanocomposite material is constituted by a matrix and a reinforcement consisting of fibers. The matrix itself comprises a resin and filler, the goal of which is to improve the characteristics of the resin while reducing the production cost. From a mechanical point of view, the filler-resin system behaves as a homogeneous material, and the composite is considered as being made of a matrix and reinforcement (Kaul et al., 2018).

2.6. Synthesis Methods of ZnO / SiO_2 Nanocomposite

The nanocomposite is synthesized through methods, depending on the end-user property demand. Synthesis of nanomaterials has two major approaches, the top-down and bottom-up approaches. Synthesis of nanocomposites has top to bottom and bottom-to-up approaches.

Top-to-Bottom Approaches were involved in the form of high-energy ball milling, severe plastic deformation, etching, mechanical alloying, lithography, reactive milling, and micromachining method. These show larger molecules make smaller to the nanoscale.

Bottom Up Approaches were involved in the form of self-assembly, Sol-gel electron or iron beam, and metal-organic. Metal-organic chemical vapor deposition, vacuum arc deposition, inert gas deposition, electrodeposition, physical/chemical vapor deposition. The bottom-up approach can be categorized into: physical, chemical, mechanical, biological, or green.

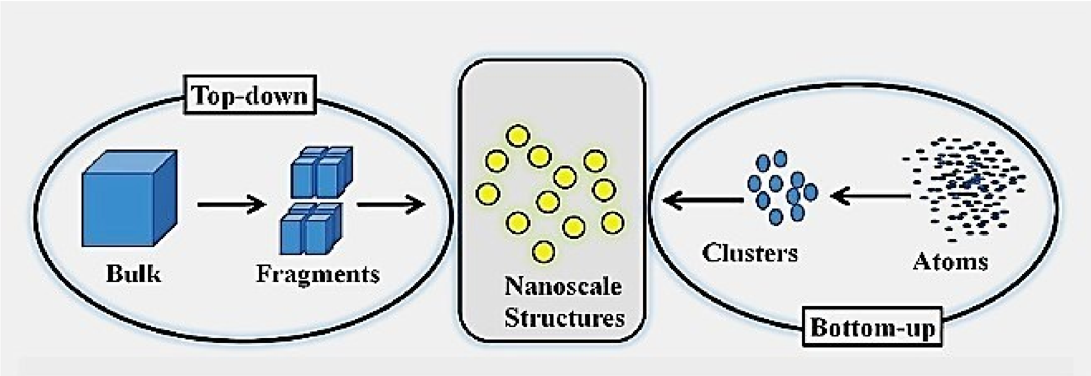

FIGURE 2: Synthesis of Nanomaterials Approaches *(Mansoori, 2017).*

2.6.1 Deposition-precipitation

By using deposition-precipitation process and acetonitrile solvent, ZnO/SiO_2 nanocomposite had created (Farrukh, 2016). In this method, two processes are involved: (i) precipitation process, it is the creation of a solid from bulk solutions or from pore fluids depending upon sufficient force of gravity (settling) to bring the solid particles together; (ii) Deposition process, it is the interaction of the precipitate particles with the support surface.

2.6.2. ZnO /SiO_2 NCs Synthesis with Green Method

Green synthesis involves the synthesis of nanoparticles by using plant extract and microorganisms such as bacteria and fungi. As reported by (Ali et al., 2019) confirmed the great impact of SiO_2 on IFT reduction and wettability alteration, consequently, increasing oil production. Alternatively, using a green and eco-friendly technique for synthesizing the nanomaterials from plant extracts can remove all the challenges of previous methods and increases the stability of the derived nanostructures by altering their sensitivity to oxygen, water, and other chemical entities.

As reported by Santhosh (Ahmed et al., 2017) ZnO NPs synthesized from the *Passiflora caerulea* leaf extract and tested against the pathogenic culture isolated from the urine of the patient suffering from urinary tract infection. The results showed that the synthesized ZnO NPs act as an antibacterial agent against urinary tract infections.

As (Bandeira et al., 2020) reported the synthesis of Zinc oxide nanoparticles from the leaf extract of *Hibiscus subdariffa*. The synthesized ZnO nanoparticles had potential anti-bacterial agents which have been studied on *Escherichia coli* and *Staphylococcus aureus*. According to the outcomes of the previous studies, the silica and zinc NPs have the same role as the surfactant. Hence, these two NPs have been combined together in a green NC, which was then coated with xanthan gum as a natural polymer to be able to modify the rheological properties and mobility ratio of Nanofluids (Ali et al., 2019).

Synthesis of ZnO/SiO_2 nanocomposite was carried out via the deposition-precipitation method by using acetonitrile solvent. The chemicals used for experimental work include Zinc Nitrate Zn $(NO_3)_2 .6H_2O$ (Merck), Tartaric acid (Panreac), liquid Ammonia (Biom), Ethanol (Biom), Silicon dioxide (DAE-JUNG), Acetonitrile (PANREAC) reported by (Nozari et al., 2021).

2.7. *Ajuga Integrifolia* Plant Description

Ajuga integrifolia Buch. -Ham. (Syn: *Ajuga remota*; *Ajuga bracteosa*) was known by common names: 'Anamura' (in Kambattic) 'Armagussa', 'Etse Libawit', and 'Medhanit' (in Amharic) (Alene et al., 2020). It was one of the species in the genus Ajuga and the family *Lamiaceae*. The plants in the genus Ajuga were evergreen, clump-forming rhizomatous annual or perennial herbaceous flowering species in the mint family, Lamiaceae (Kaur, 2018). There were at least 301 species of the genus Ajuga with many variations. Ajuga was one of the 266 genera of the family Lamiaceae (Vohra and Kaur, 2011). *Ajuga integrifolia,* mostly known under the name *Ajuga bracteosa*, was an herb often lying on the ground and rooting at the nodes, covered with soft hairs, and stems growing up to 40 cm high. Its leaves were coarsely toothed. Its flowers are small, pale blue, white or pale violet found in small clusters in the leaf axils. It flowers from late August to October while honeybees were frequently visiting the flowers for pollen and nectar (C. Science, 2019) regional state, Kanbatta Timbaro (K.T) Zone Durame town 328km from Addis Ababa.

FIGURE 3: *Ajuga integrifolia* (Jayachandran et al., 2021).

2.8. Antibacterial Activity of Nanoparticles

2.8.1. Antibacterial Activity of Zinc Oxide (ZnO) Nanoparticles(NPs)

Zinc oxide possesses some antibacterial effects, good thermal qualities, and color stability, with low cost and little toxicity. The noble gas electronic configuration of zinc in ZnO NPs is one reason for its low toxicity and less antibacterial activity. Because of its full electronic configuration, it is stable and cannot easily bind to electron donor groups in biological molecules containing sulfur, oxygen, or nitrogen. The antimicrobial activities of zinc oxide nanoparticles in contact with bacteria and fungi are shaped by particle sizes, morphologies, concentration and specific surface areas involved, with smaller particles offering better inhibitions in higher concentrations (Liu & Chen, 2022). The antimicrobial activity of synthesized Zinc oxide nanoparticles studied against three microbial strains *E. coli, Salmonella, Acetobacter* and their zone of Inhibition obtained at a different concentration of zinc oxide nanoparticles are shown in the table blow.

TABLE **1:** Zone of inhibition observed at different dilutions of ZnO NP

Microbial strains	The diameter of the Zone of inhibition observed at different dilutions of ZnO NPs(in mm)			
	25%	50%	75%	100%
Acetobacter	9	10	11	12
E.coli	11	11	12	13
Salmonella	11	12	15	17

2.8.2. Antibacterial Activities of ZnO/SiO_2 NCs

The antibacterial activity of ZnO is well-known and the combination of ZnO with SiO_2 nanocomposites can enhance its antibacterial efficacy. Many studies have reported the antibacterial application of ZnO/SiO_2 nanocomposites against various bacterial strains, including *Escherichia coli, Staphylococcus aureus,* and *Pseudomonas aeruginosa*. ZnO/SiO_2 nanocomposites are attributed to the release of Zn^{2+} ions from the ZnO component, which can affect the bacterial cell membrane and inhibit bacterial growth. Additionally, ZnO/SiO_2 NCs have also been investigated for their potential use in biomedical applications such as tissue engineering and drug delivery, in case of their biocompatibility and easy use. But it is essential to take major that the potential cytotoxicity of ZnO nanoparticles, including those incorporated into ZnO/SiO_2 nanocomposites, should be carefully evaluated before their wide distribution to use in antibacterial applications.

2.8.3. Photocatalytic Activity of ZnO NPs

Zinc oxide (ZnO) nanoparticles (NPs) have been widely studied for their photocatalytic activity. When exposed to light, ZnO NPs can generate electron-hole pairs, which can initiate photocatalytic reactions. This property of ZnO NPs makes them attractive for a range of applications, including environmental remediation, water purification, and solar cell technology (Balcha et al., 2016).

The photocatalytic activity of ZnO NPs is dependent on a number of factors, including the size and morphology of the particles, the surface area-to-volume ratio, and the bandgap energy of the material. Smaller particles tend to exhibit higher photocatalytic activity due to their increased surface area-to-volume ratio and the greater likelihood of electron-hole pair generation. Additionally, ZnO NPs with a higher degree of crystallinity tend to exhibit higher photocatalytic activity (Alosaimi et al., 2021) .

ZnO NPs have been shown to be effective in photocatalytic degradation of a range of pollutants, including organic dyes, pesticides, and pharmaceuticals. In addition, ZnO NPs have been used for the production of hydrogen through water splitting and for the degradation of organic pollutants in wastewater treatment (Mohamed et al., 2012).

Overall, the photocatalytic activity of ZnO NPs makes them a promising material for a range of applications, particularly in the fields of environmental remediation and energy conversion. However, careful consideration must be given to the potential health and environmental impacts of the use of these nanoparticles (Surakasi et al., 2022).

2.8.4. Photocatalytic Application of ZnO/SiO_2 NCs

The unique characteristics of ZnO/SiO_2 nanocomposites, such as their high surface area, improved light absorption, and effective electron-hole separation, have led to substantial research on them as photocatalysts (Alosaimi et al., 2021) .

ZnO/SiO_2 nanocomposites have demonstrated remarkable results in photocatalytic applications when it comes to the breakdown of several organic contaminants like phenol, methylene blue, and rhodamine B under UV light irradiation. The synergistic interaction of

ZnO and SiO_2, where SiO_2 serves as a support for ZnO nanoparticles, limiting their agglomeration and boosting their stability, is responsible for the photocatalytic activity of ZnO/SiO_2 nanocomposites (Ren et al., 2021).

SiO_2 can also increase the reusability of ZnO/SiO_2 nanocomposites, which makes them more practical for use in large-scale applications. ZnO/SiO_2 nanocomposites can also have their surface modified with other functional groups or doped with additional substances like sulfur or nitrogen to increase their photocatalytic activity (Eletta et al., 2018).

ZnO/SiO_2 nanocomposites have a great deal of potential as photocatalysts for applications in environmental remediation, and by enhancing their surface characteristics and composition, their performance can be further enhanced.

2.9. Methylene Blue Dye Elimination

Methylene blue (MB) is a normally used dye in textile, paper, and leather-based industries. Its presence in wastewater can reason environmental problems and damage aquatic lifestyles. MB dye removal methods are adsorption, photocatalysis, membrane filtration, biological treatment, and chemical oxidation (Maijan et al., 2020).

2.9.1 Adsorption

Adsorption is an extensively used approach for MB dye elimination. Adsorbents that contains activated carbon, zeolites, and various forms of nanoparticles had been used for MB adsorption. The adsorption method is stimulated by way of different parameters such as pH, temperature, and the floor location of the adsorbent (Maijan et al., 2020).

2.9.2 Photocatalysis

Methylene blue dye photocatalytic degradation using semiconductors such as ZnO, CdS, and TiO_2 has been supported in the review literature. In the UV light irradiation, the photocatalytic degradation produces reactive oxygen that decompose the MB dye into smaller, less harmful compounds and less toxic (Nazarkovsky et al., 2021).

2.9.3. Membrane Filtration

Methods those used in membrane filtration are ultrafiltration and nano filtration can remove MB from wastewater. The membrane filtration efficiency depends on the size and charge of the MB molecules and the membrane pore size (Balcha et al., 2016).

2.9.4. Biological Treatment

Using microorganisms such as bacteria and fungi can effectively remove MB from wastewater is said to be Biological treatment. The microorganisms break down the dye molecules into less harmful substances (Faisal, Jan, Shah, Shah, Khan, Akbar, Rizwan, Jan, Akhtar, et al., 2021).

2.9.5. Chemical Oxidation

This method produces highly reactive hydroxyl radicals that degrade the MB dye into smaller, less harmful compounds. The Chemical oxidation methods include Fenton's reagent, and advanced oxidation processes (AOPs) have been important for MB dye removal (Senthil Kumar et al., 2019).

CHAPTER THREE

3. Materials and Methods

3.1. Study Sites Descriptions

Green Synthesis of ZnO NPs, and ZnO/SiO_2 NCs done by using *Ajuga integrifolia* medicinal leaf extract and their antibacterial, and photocatalytic activity were evaluated and characterized in the Applied Chemistry Laboratory of Adama Science and Technology University (ASTU). Some characterizations were performed in different places due to the lack of some instruments. UV-Vis spectrophotometer (p9 Double Beam UV-Visible Spectrophotometer, made in China UQS2102010) characterization was performed in Applied Chemistry laboratory ASTU, and the morphology of the synthesized nanostructures were studied via scanning electron microscopy (SEM, Hitach S4800, Japan) characterization was performed in South Korea. X-ray diffractometer (XRD-700 Shimadzu Co., Japan,$\lambda CuK1=0.15406$ nm, tube Voltage 40 KV, current 30 mA), characterization was carried out in the materials science engineering laboratory, and Fourier transform infrared (FTIR) spectrometer was used to the formation of NPs and the existence of functional group (Jasco, FT/IR-6600, Japan) performed in Bahir Dar university. Evaluation of antibacterial activity was done in the biology laboratory in a school of applied natural science. The plant *Ajuga integrifolia* was collected from Southern Ethiopia of S.N.N.P.R.S.

3.2 Collection of *Ajuga Integrifolia* Plant Leaves

Ajuga integrifolia leaves were collected from around Shinshicho Town, in Kachabira woreda, located in Kambatta (K) Zone, S.N.N.P. Region, in Ethiopia. It was located between latitudes 7.08 – 7.30^0 N and 37.22– 38.04^0 E longitude, and topographically the Zone lies between altitudinal ranges of 501m above sea level and 3080m above sea level. The leaf samples were washed several times with tap water followed by distilled water to remove extraneous matter. The cleaned leaves were completely dried at room temperature in the opened air and under shadow for two weeks (15 days) on the aluminum foil. The dried leaves were crushed by using an electrical grinding machine (grinding machine) then after a fine powder was produced and packed in a brown bottle to protect against the effect of light.

3.3. Chemicals

All the chemicals and reagents used for the preparation of ZnO/ SiO_2 NCs were purchased commercially from local chemical markets. Zinc acetate was used as a precursor to synthesize the ZnO/SiO_2 NCs and Tetraethylorthosilicate (SRL-Tetraethyl Orthosilicate

(TEOS) extra pure,98%,28-28.8%SiO_2 500ml-93314 made in India.) was used as a precursor of silicon dioxide nanoparticles. Zinc acetate (Zn (CH_3COO) $_2$.2H_2O, 98% extra pure, supplier Thermos Scientific) was used to synthesize zinc nanoparticles, distilled and tap water (H_2O) was used to remove dirt from *Ajuga integrifolia* leaf, as solvent dimethyl sulfoxide (DMSO 99.9% pure made in EU.) was used to disperse ZnO/ SiO_2 NCs. Sodium hydroxide (NaOH, purists. P.a., ACS reagent, reag, Ph, Eur., K ≤0.02%, ≥98%, pellets, supplier Thermo Fisher Scientific) was used to adjust pH, the Aluminum foil was used to cover the plant extract to prevent from sunlight, TEOS was used as a precursor for SiO_2 NPs, leaves of *Ajuga integrifolia* medicinal plant was used to stabilize product as capping agent. All aqueous solutions were prepared using distilled water. The bacterial strains were used for checking the antibacterial activity synthesized materials against Gram-positive (*Staphylococcus aureus)* and Gram-negative *(Escherichia coli).*

3.4. Method

3.4.1. Preparation of Plant Leaf Extract

The leaves of *Ajuga integrifolia* would be used for the study were detached from the parent plant and washed with tape water to remove dust particles and other waste material from the surface of the leaves. The leaves were placed in a shaded and opened place at room temperature for 15 days then after dried in the fresh air without exposing sunlight and heat. The air-dried leaves of *Ajuga integrifolia* were chopped into small pieces and milled into a uniform powder by an electrical grinder. A. *integrifolia leave* extract was obtained through a boiling mixture of 15 gm of finely grounded A. *integrifolia* and 300 mL double distilled water in a 500 mL conical flask for 60 minutes and to 60 ^{0}c under constant stirring. After this process, the extracts were cooled at room temperature, filtered, and used as a mediating agent for the synthesis of nanomaterials. The extract was stored in the refrigerator until to use.

3.4.2. Synthesis of Zinc Oxide NPs Using *Ajuga Integrifolia* Leaves Extract

100 mL of 0.1 M of Zinc acetate dehydrate was added to the extract of 50 ml as the temperature reached 60 °C. The mixture was heated to 80 °C upon continuous stirring for 2 hours in a 250 ml beaker. Then, the solution pH was adjusted to 12 using 0.1 M NaOH when 30 min. remain to finish the given time, and white ZnO NPs precipitate formed. The as-prepared ZnO NPs were collected via decantation, washed with double distilled water, and dried in the oven at 80 ^{0}C for 1 hour. The dried ZnO NPs were characterized and used for applications.

3.4.3. Synthesis of SiO_2 NPs Using *Ajuga Integrifolia* Leaves Extract

20 ml of Tetraethylorthosilicate (TEOS) was added dropwise to 100 mL of freshly prepared A. *integrifolia* leaf extract while the mixture was being stirred at 60˚C. The procedure was carried out under reflux conditions for 12 hours at pH 9 until the SiO_2 NPs was formed. The pH value of the solution was adjusted to increase precipitation using 0.1 M NaOH. The centrifugation at 3500 rpm for 50 minutes separated the residues from the mixture, and washed carefully with distilled water twice, and once finally with ethanol to remove all contamination, and finally dried in the oven at 80 ^{0}C for 2 hours. Inserted the dried powder into furnace then calcinated at 550 ^{0}C for 60 minutes. Then after the fine powder was kept for further characterization and application activities.

3.4.4. Green Synthesis of ZnO/ SiO_2 NCs Using *Ajuga Integrifolia* Leaf Extract

A 100 ml of 0.1M Zn $(CH_3COO)_2.2H_2O$ aqueous solution, 50 mL aqueous extract of *Ajuga integrifolia*, and 2ml TEOS were mixed and vigorously stirred for 30 min at room temperature. During this time, the color of the contents of the flask was changed from light brown to white. The mixture was heated to 80 °C upon continuous stirring for 2 hours. Then, the solution pH was adjusted to 12 using 0.1 M NaOH before finished the stirring just 30 minute remains and white ZnO/SiO_2 NCs precipitate formed. The obtained white precipitates were centrifuged at 3500rpm. The particles precipitated at the bottom of the container was filtered, washed with double distilled water, dried at room temperature, and inserted the filtered NCs by putting in crucible dish in the Oven at 80 ^{0}c temp. for 2 hours, then after the dried powder crushed by mortar and finally fine powder obtained was kept to use for experiments (Purohit et al., 2020).

CHAPTER FOUR

4. Result and Discussion

4.1 UV-Vis Spectrophotometer Analysis

The pattern of absorption spectra generally depends on the parameters such as the method of synthesis, temperature, size, and shape of the NPs synthesized. The absorption maxima of A. *Integrifolia-assisted* synthesized ZnO NPs occurred around 351.4 nm as shown in (Fig.4 a.) which is in agreement with the previous report. The absorption maxima for ZnO bulk usually occurs around 369 nm (Jamdagni et al., 2016) . These blue-shift absorption maxima from the bulk ZnO confirms the formation of ZnO NPs.

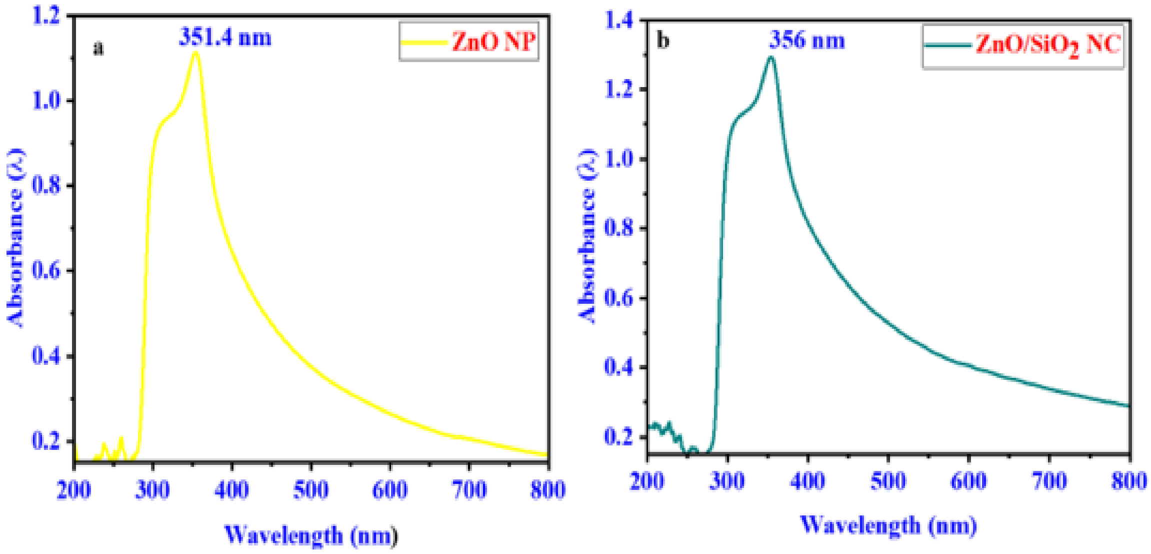

FIGURE 4: (a). UV-Vis spectrophotometric result of ZnO NP and (b) ZnO/SiO_2 NCs

The absorption maxima of A. *Integrifolia-assisted* synthesized ZnO/SiO_2 NCs occurred around 356 nm as shown in (Fig.4 b.) above. The green-produced composites had higher absorption peaks than ZnO NPs, according to the ZnO/SiO_2 NC absorption maxima. These blue-shift absorption maxima from the bulk ZnO increased with the addition of SiO_2 NPs. Therefore, the green synthesized ZnO/SiO_2 NCs confirm the presence of SiO_2 NPs increases the size of absorption of ZnO/SiO_2 NC. The UV peak increased in ZnO/SiO_2 NC due to oxygen vacancies, surface traps, and interstitial structural defects (P. K. Sharma et al., 2009). The near absence of visible emission in the case of Fig 4 b is due to larger interactions of the surface states with the SiO_2 matrix (Panigrahi et al., 2011).

4.2 FTIR Spectra of Green Synthesized *Ajuga Integrifolia*, ZnO NPs, and ZnO/SiO_2 NC

The unique band centered from 412-433cm^{-1} corresponding to Zn–O stretching vibration which confirms the green synthesis of ZnO nanoparticles (Sekhar et al., 2019). The FTIR study also confirmed the result of the preliminary phytochemical investigation discussed that proteins, phenolic compounds, and alcoholic compounds present in A. *integrifolia* extract acted as a reducing agent and stabilizing agent in the formation of ZnO NPs and further prevented its agglomeration.

The peak 860 cm^{-1} corresponds to the bending vibration, reflecting the characteristics of SiO_2. The Si-ZnO bond formation was confirmed by reduction in peak intensity at 450 cm^{-1} –500 cm^{-1} of Si-O-Si (Jayachandran et al., 2021). The absorption peak at 2360 cm^{-1} is the C=O stretching mode vibrations which is indicating the adsorption of atmospheric CO_2 on the nanocomposite's surface (Ali et al., 2019).The absorption peaks at 1414 and 1486 cm^{-1} are the stretching vibrations of C-O and C=O bonds of the carboxyl group respectively. The absorptions at 1040 cm^{-1} is due to the dissymmetric vibration of Si-O-Si (Rahimzadeh et al., 2022). The absorption peak at 561 cm^{-1} shows the stretching vibrations of the Si-O bond (Spoiala et al., 2014). The absorption peak at 437 cm^{-1} is attributed to the stretching vibrations of Zn-O (Kokabi et al., 2017). The nanocomposite ZnO/SiO_2 showed strong bands near 1063 cm^{-1}, which can be attributed to the asymmetric stretching vibrations of the Si-O-Si group. The absorption bands at 3201, 3338, and 3345 corresponded to ZnO NPs, A. *integrifolia*, and ZnO/SiO_2 NCs respectively are OH stretching indicators shown in figure 6. As illustrated in figure 6. absorption bands at 1569, 1582, and 1596 cm^{-1} determined from the IR spectra of A. *integrifolia,* ZnO/SiO_2 NCs, and ZnO NPs revealed the stretching and bending vibration groups of the H_2O molecule respectively.

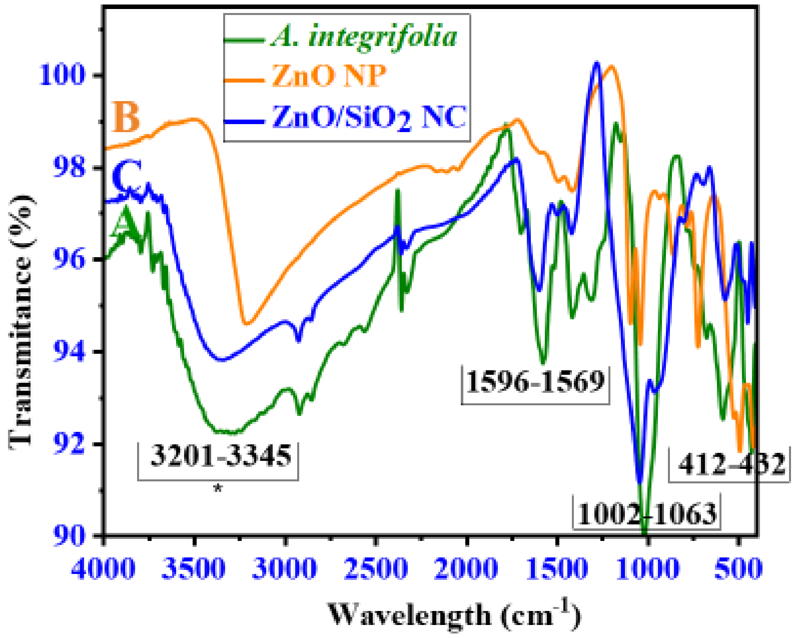

FIGURE 5: FTIR spectrometric result of (A) *Ajuga integrifolia* (B) ZnO NPs, and (C) ZnO/SiO_2 NCs

4.3 X-Ray Diffraction (XRD) Analysis

The crystalline nature of ZnO (2:1) NPs was investigated by XRD and the pattern shows peaks at $2\theta = 31.9, 35.18, 36.32, 47.72, 56.83, 62.99, 66.64, 68.12$, and $69.15°$ corresponding to lattice planes (100), (102), (101), (102), (110), (103), (200), (112), and (201), respectively, which indicated that the samples were crystalline Wurtzite ZnO structure (JCPDS Card no: 36–1451). Fig 6 a. shows sharp peaks of ZnO which indicate the crystallinity in nature. This further proves that the produced powder is pure ZnO NPs because no peaks associated with any intermediary substances or contaminants were seen (Safawo et al., 2018). The narrow and strong peaks indicate the NPs have good crystallinity and size. The synthesized ZnO NPs crystallite size was calculated using Debye-Scherrer's formula (A. Sharma et al., 2012), and the average crystallite size of the sample was estimated to be 20.886 nm which is derived from the FWHM of the most intense peak corresponding to (100) plane located at 36.35°. The calculated average size of particle is small enough and close to Zincite (ZnO). The XRD pattern of synthesized ZnO (3:1) NPs showed peaks, where the three intense peaks found at 36.37^0,34.5349^0, and 31.8824^0, corresponding to the (100,102, and 101 planes respectively. Thus the below mentioned table 3: had larger average size in ZnO (3:1) covered of 24.35 nm than ZnO (2:1) NPs.

The crystalline nature of SiO_2 NP was investigated by XRD and the pattern shows peaks at 2θ= 21.1396 ^{0}, 20.5612^0, and 22.9353 ^{0}. The increase in the peak width of the XRD indicated an amorphous state. The above-mentioned peaks were typical for the SiO_2 structure (JCPDS # 43-596) in Fig 6 C. The three strongest peaks, which correspond to the (140), (126), and (118), respectively, were identified at 21.1396, 20.5612, and 22.9353 in the XRD pattern of synthetic SiO_2 NPs. The result indicated that SiO_2 NPs produced using green synthesis method has amorphous nature.

The crystalline nature of ZnO/SiO_2 NC was investigated by XRD and the pattern shows peaks at 2θ=36.32^0, 31.78^0, and 34.55^0 corresponding to lattice planes (100), (002), and (101) respectively which indicate the sample peak intensity, position and width. The appearance of additional peaks other than SiO_2 peaks at 45.98^0, 56.46^0, 62.84^0.and 68.46^0 indicates the presence of ZnO nanoparticles. The crystallite size of ZnO/SiO_2 was calculated to be 8.1737 nm according to Scherrer's equation. It is observed that the crystallite size was decreased by adding silica in the precursor. It was caused by a decrease in the zinc precursor concentration after adding an amount of silica (Justine et al., 2019).

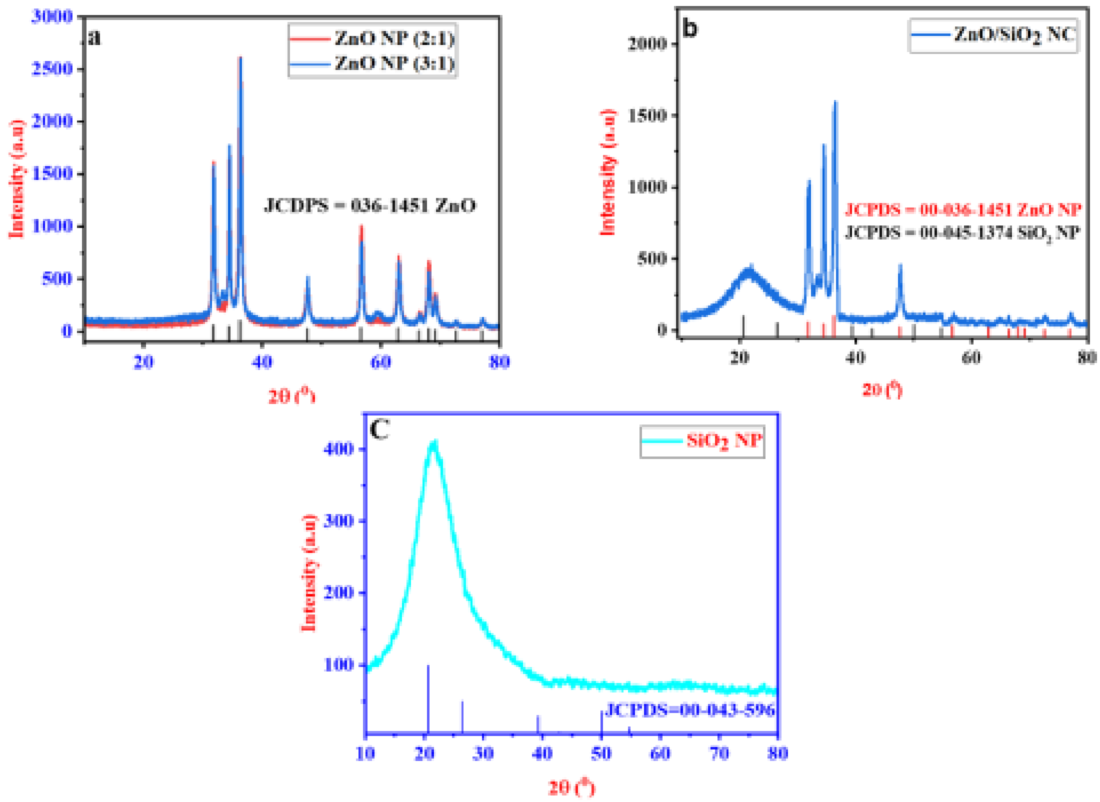

FIGURE 6:XRD results of (a) ZnO (2:1 & 3:1) NPs, (b) ZnO/SiO2 NC, and (c) SiO_2 NP

TABLE **2:**The Crystalline size & parameter value of green synthesized ZnO (2:1) NPs

2θ	FWHM	FWHM In rad	Cos Theta	Average size (nm)	D-spacing (nm)	Lattice parameter, Â	hkl
36.35	0.451	0.0078	0.955	20.886	19.365	19.365	100
34.51	0.3609	0.0062	0.955		24.076	10.767	102
31.86	0449	0.0078	0.961		19.219	13.589	101

Table 2: Shows a summary of parameters extracted from the XRD spectra of the green synthesized ZnO NPs. The calculated average size of this particle is small enough and close to Zincite (ZnO). The XRD pattern of synthesized ZnO (2:1) NPs showed peaks, where the three intense peaks found at 36.35^0, 34.5129^0, and 31.8608^0, corresponding to the (100, 102, and 101 planes respectively.

TABLE 3:The crystalline size & parameter value of green synthesized ZnO (3:1) NPs

Peak position	FWHM in Rad	Cos theta	An average size in nm	D-spacing in (nm)	Lattice Parameters Â	hkl
36.3763	0.0061648	0.950086	24.356	22.30941	22.309415	100
31.8824	0.006206733	0.961582		22.4270	10.029659	102
34.5349	0.004879211	0.954974		28.3328	20.034381	101

TABLE 4: The Crystalline size and parameter value of green synthesized ZnO/SiO_2 NCs

Peak position(2θ)	FWHM in Rad	Cos theta	Average size in nm	D-spacing in (nm)	Lattice parameters Â	hkl
36.3217	0.01413	0.950235319	8.17376	9.73503	9.73503	100
31.7862	0.020061	0.961812794		6.94039	3.470195	002
34.5533	0.01761	0.954927298		7.845856	5.547857	101

Table 4: mentions that the green synthesized ZnO/SiO_2 NCs properly decreased the size of the peaks because the presence of SiO_2 NPs. In general, the green synthesized ZnO/SiO_2 NCs were effective, as shown in Table 4 above, with calculated an average size of less than that of the ZnO NPs in Table 2 and 3.

4.4 SEM Analysis

SEM analysis was used to determine the morphology of the produced nanopowders of ZnO and ZnO/SiO_2 NCs (Durgude et al., 2022). Figure 7 (a, b) represent SEM image of ZnO NPs, and Figure 7 (c, d) represent SEM image of ZnO/SiO_2 NC, SEM image showed that the created nanoparticles and nanocomposite are spherical in shape. SEM image revealed due to addition of distilled water and TEOS nanoparticle agglomeration was increased (Safavinia et al., 2021). The morphology of ZnO nanoparticle contained an irregular shape, when silica was added.

The SEM analysis of green synthesized ZnO NPs and ZnO/SiO_2 NCs revealed a spherical shape. The SEM micrograph was shown that the larger particles mostly consist of silicon and oxygen and the flakes are mostly made up of zinc and oxygen. The ZnO/SiO_2 nanocomposite was shown the spherical morphology with highly porous structure (Sekhar et al., 2019). According to the morphology of the SEM images shown by the authors (Mao et al., 2021), the shapes of ZnO, and ZnO / SiO_2 with various sizes below 100 nm were observed. It can be seen that the particles were developed together in cluster formations, and are randomly distributed.

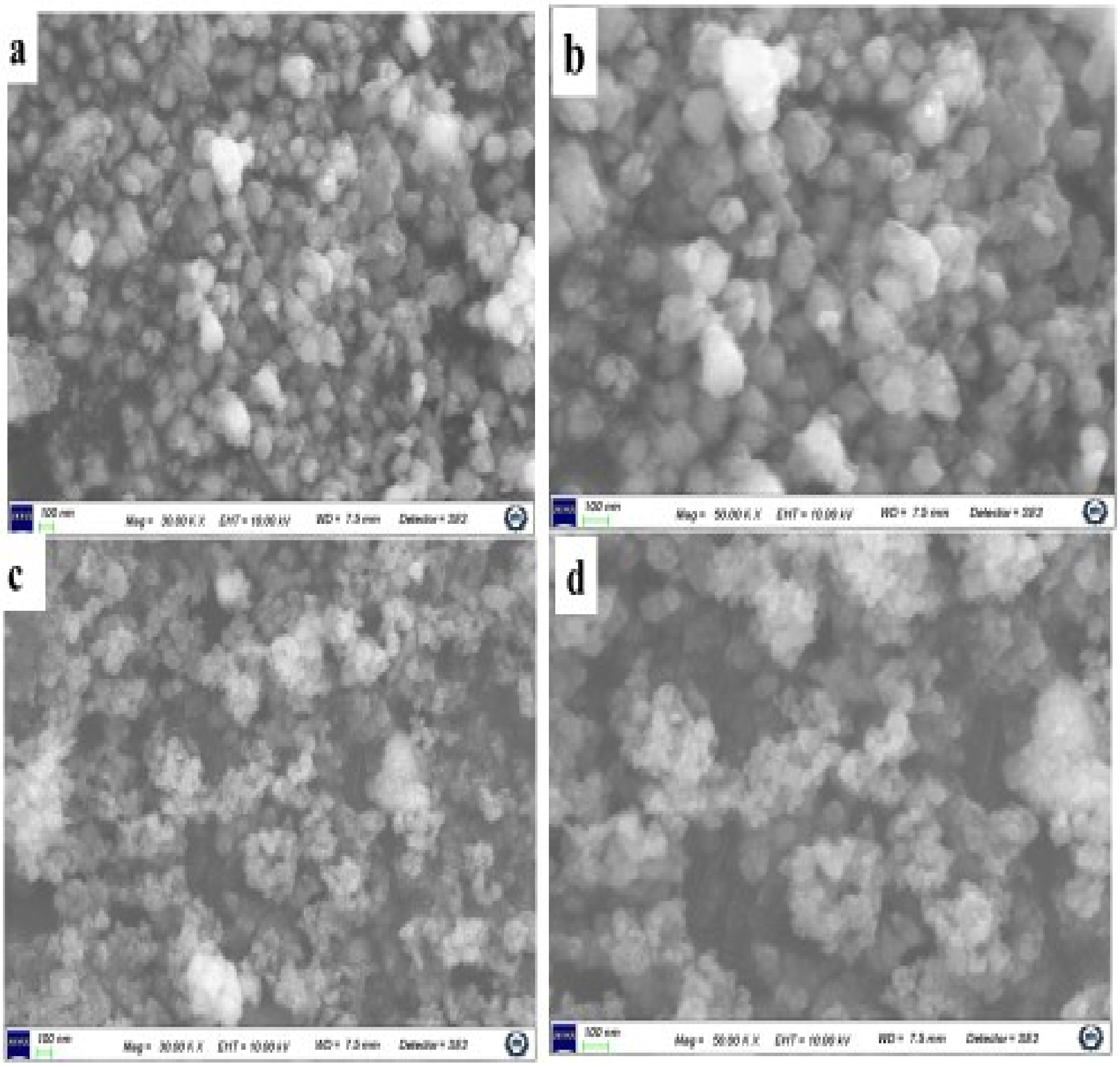

FIGURE 7: SEM images at 100 nm of (a, b) ZnO NPs, and (c, d) ZnO/SiO_2 NCs

4. 5 Antibacterial Activity

4.5.1. Disk Diffusion Methods

To test their antibacterial effect antibacterial studies of the synthesized nanocomposite were carried out on four bacterial strains; E. *coli* (E. C), and *Staphylococcus aureus* (S.A.) *Streptococcus pyogenesis* (S. PY), and *Pseudomonas aeruginosa* (P.A) which were obtained from the Microbiology laboratory of ASTU. The study was carried out by using the disc diffusion method. In this study, A. *integrifolia* extract-mediated synthesized ZnO NPs and ZnO/SiO_2 NC exhibited antibacterial activity against all tested pathogenic gram-negative, and gram-positive bacteria.

The antibacterial activity of green synthesized ZnO NPs and ZnO/SiO_2 NC were investigated with four different concentrations (12.5, 25, 50, 100 mg/ml) against Gram-positive

(*Staphylococcus aureus*, and *Streptococcus Pyogenesis)* and Gram-negative bacteria (*E. Coli*, and *Pseudomonas aeruginosa)* by agar disk diffusion method and the results are shown in (Fig. 8, fig. 10, and Table 4 & 5). Among the tested pathogenic strains, *Staphylococcus aureus* and *Streptococcus pyogenesis* exhibited higher sensitivity to ward ZnO NPs with (15 mm) and (17 mm) zones of inhibition, while *E. coli* and *Pseudomonas aeruginosa* exhibited the least sensitivity with (12 mm) and (6 mm) zones of inhibition at 100 mg/mL, which implies that Gram-negative bacteria seemed to have more resistance to ZnO nanoparticles. In general, Pseudomonas aeruginosa hadn't sensitivity in terms of ZnO NPs with (6 mm) zone of inhibit at 100, 50, 25, and 12.5 mg/ml concentrations respectively. Meaning *pseudomonas aeruginosa* had resistance to ZnO NPs. When tested, gram-positive bacteria (*Staphylococcus aureus* and *Streptococcus pyogenesis*) and gram-negative bacteria (*E. coli* and *Pseudomonas aeruginosa*) exhibited higher sensitivity to ward ZnO/SiO_2 NCs with (15, 20, 20, and 16 mm) zones of inhibition at 100 mg/ml, which implies that both gram-negative and positive bacteria showed no resistance to ZnO/SiO_2 NCs. In general, the compound ZnO/SiO_2 proved more efficient than ZnO NPs. The difference in sensitivity between gram-negative and gram-positive bacteria could be due to morphological differences, which result in variable resistance to nanoparticle invasion through bacteria walls. The antibacterial activity of ZnO/SiO_2 NCs is also connected to their physiochemical features, such as size, shape, chemical composition, and solubility. Because of their increasing accumulation inside the cell membrane and cytoplasm, the size of the NCs may have a greater impact on their bioactivity.

TABLE **5:** Antibacterial activity of green synthesized ZnO NPs

Sample code	Concentration In (mg/ml)	*Escherichia coli* (E.C)	*Psoudonones aeruginosa* (P.A)	*S. aureus* (S.A)	*Streptococcus Pyogenesis* (S.PY)
		Inhabitation zone (mm)	Inhabitation zone (mm)	Inhabitation zone (mm)	Inhabitation zone (mm)
ZnO NP	100	12	6	15	17
	50	13	6	11	14
	25	10	6	8	7
	12.5	8	6	7	11
	+ control	30	28	29	29

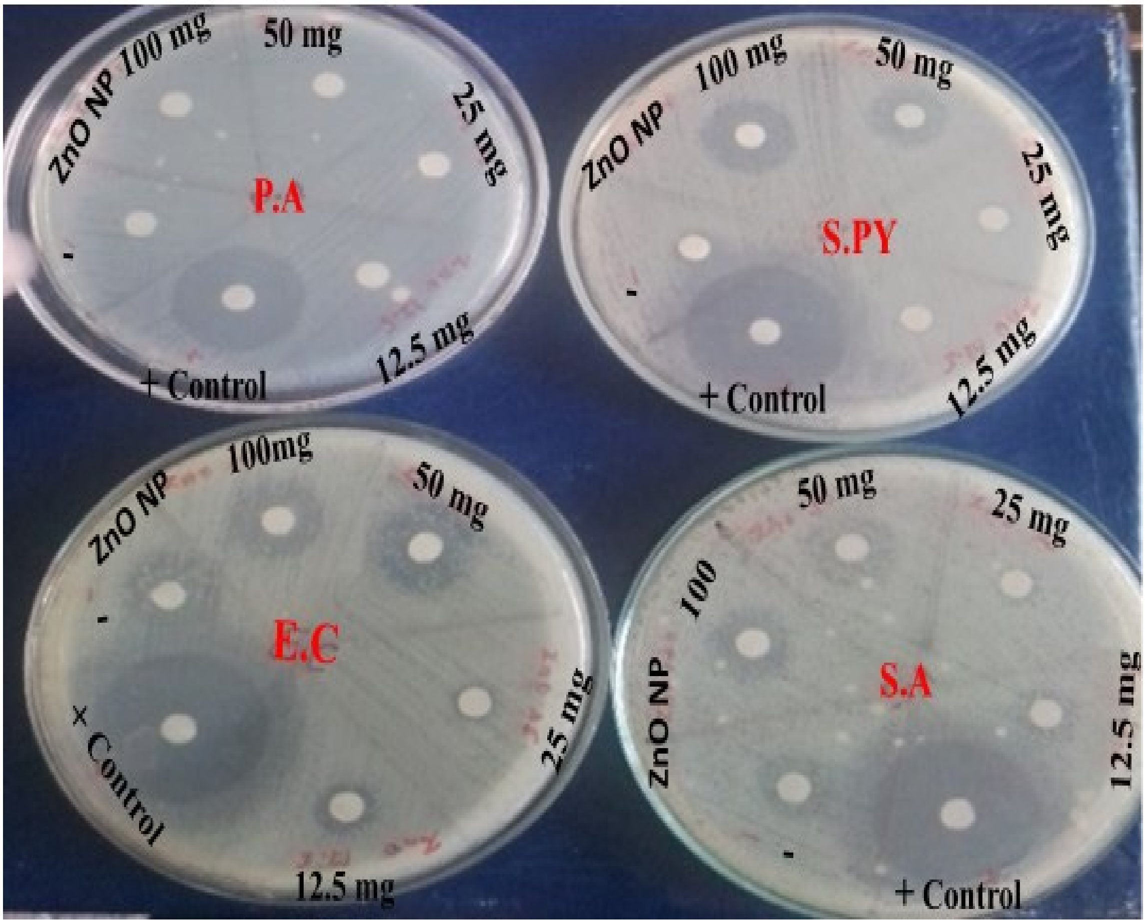

FIGURE 8: ZnO NPs antibacterial activity

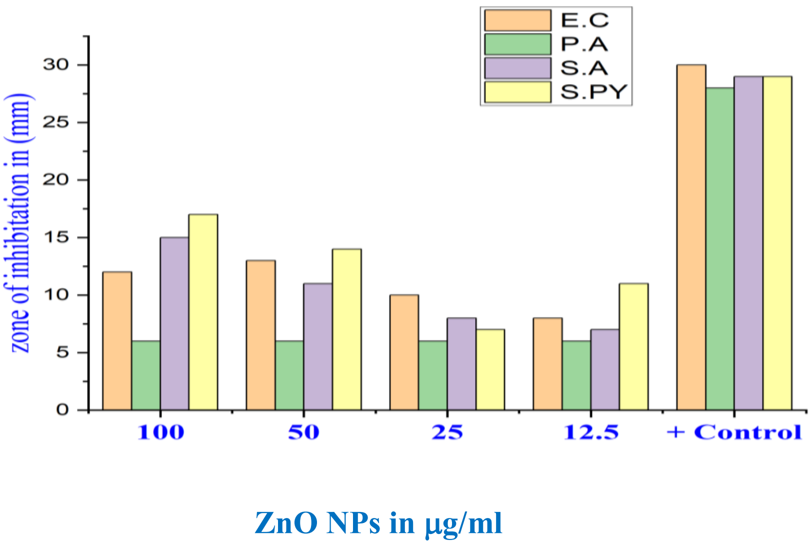

FIGURE 9 : Graphically antibacterial activity of ZnO NPs in mg/ml

TABLE **6**: Antibacterial activity of green synthesized ZnO/SiO_2 NCs

Sample code	Concentration In (mg/ml)	*Escherichia coli (*E.C)	*Psoudonones aeruginosa* (P.A)	*S. aureus* (S.A)	*Streptococcus Pyogenesis* (S.PY)
		Inhabitation zone (mm)	Inhabitation zone (mm)	Inhabitation zone (mm)	Inhabitation zone (mm)
ZnO/SiO_2 NC	100	20	15	15	20
	50	15	10	14	12
	25	14	6	11	11
	12.5	13	6	8	8
	+ Control	28	25	30	30

Antibacterial Mechanisms: collision between negatively charged cell wall and positively charged zinc oxide ions, formation of photo generated ROS and free radicals (Sportelli et al., 2022). Thus, antibacterial activity through several mechanisms exerted ZnO NPs: release of ZnO NP, the electrostatic force of interaction between ZnO ions and bacterial cell wall, production of free radicals and ROS, and surface area.

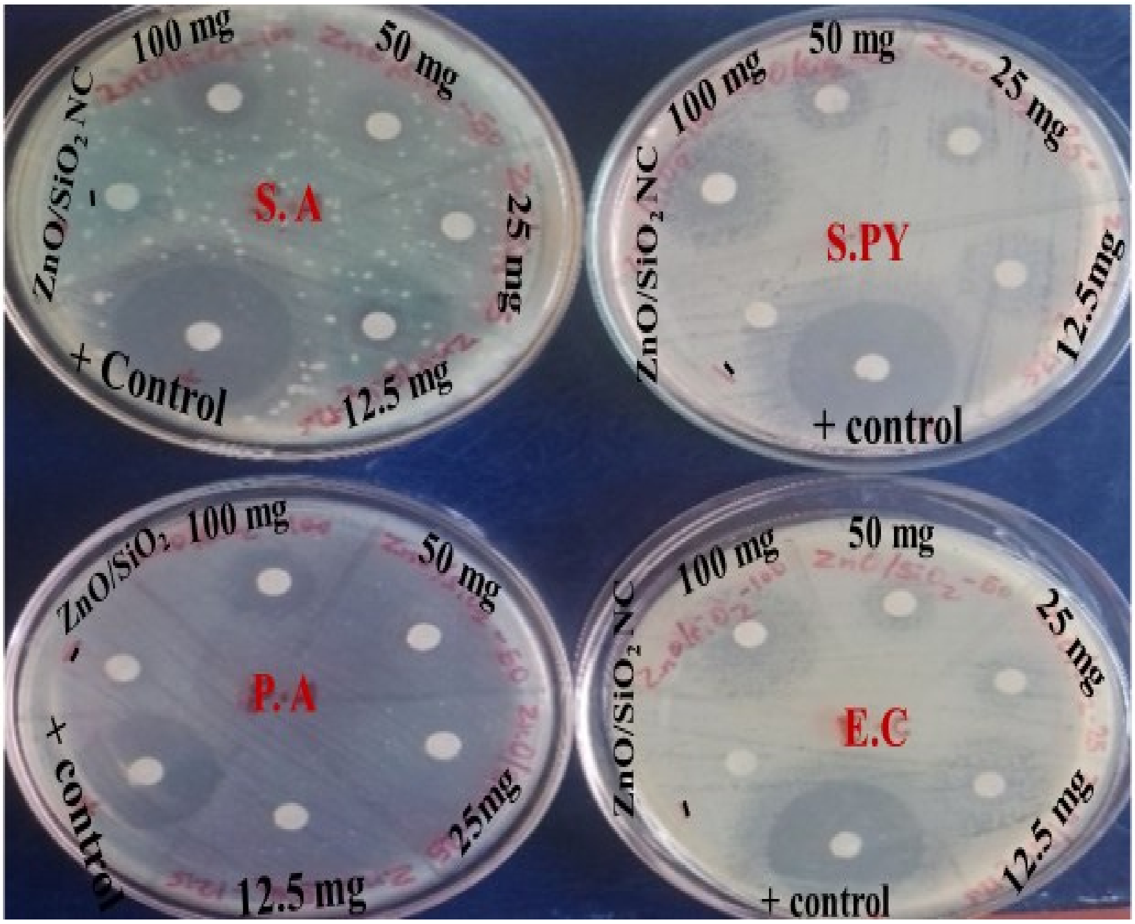

FIGURE 10: ZnO/SiO_2 NCs antibacterial activity

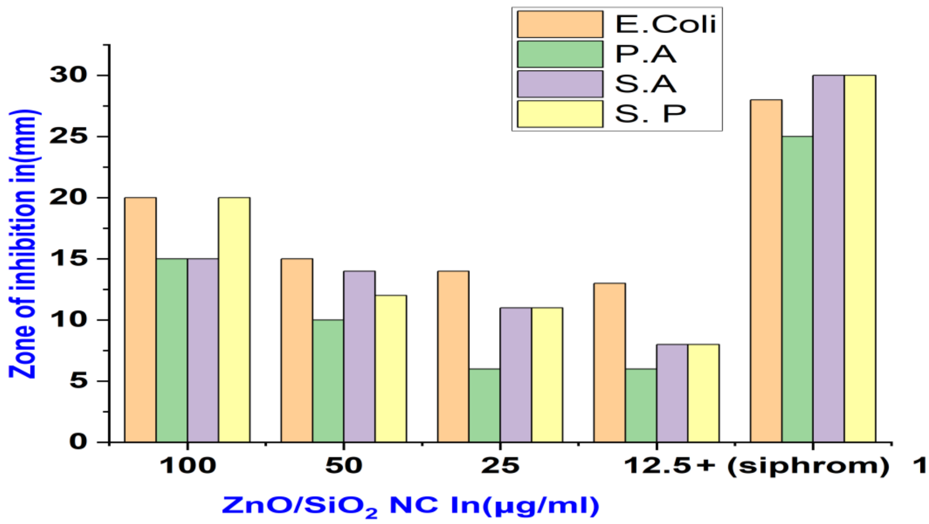

FIGURE 11: Graphically antibacterial activity by ZnO/SiO_2 NCs

4.6 Degradation of Methylene Blue Dye Solution

4.6.1 Effect of pH of Methylene Blue Dye Solution

The pH result of dye solution has an important role in the degradation process, which affects the charge properties of the surface (Hassan et al., 2022). The photocatalytic degradation of methylene blue dye using the synthesized ZnO and ZnO/SiO_2 NC were investigated at various pH (3, 6, 7, 9, and 11) while other parameters were kept as it is,100 ml of 25 ppm of MB solution by adding 100 mg of catalyst in to the solution for 30 minutes of open Sun-light irradiation in figure 12 (A). It was observed that at pH 3-6 degradation of MB dye increased, however after pH 6 the degradation of MB was decreased. The high amount of dye degradation was observed at pH 6 and it is optimum pH for this reaction using ZnO/SiO_2 NC, because behind this value, the degradation efficiency is decreased. When the pH was acidic, the positive charge of the surface attained the negative charge, then after negative surface attracts the cationic dye because of electrostatic attraction between cationic (ZnO/SiO_2 NC) and anionic species (Alosaimi et al., 2021).

The photocatalytic activity of ZnO/SiO_2 NC was evaluated by the degradation of methylene blue (MB) dye under visible light irradiation; the results indicated 97.5% degradation efficiency of MB by using pH 6, 75 mg of catalyst, 25 ppm concentration of dye, and 30-minute open sun light irradiation. The degradation efficiency of MB dye by using ZnO NP was obtained 95%.

4.6.2. Effect of Catalyst Dosage

Dye degradation is dependent on the catalyst load, the photocatalytic activity of ZnO/SiO_2 NCs was evaluated by varying the amount of catalyst from 25 mg, 50 mg, 75 mg, and 100 mg in 100 ml and 25 ppm of dye solution with 30 minutes' open sun light irradiant, pH also assigned at 6 which is optimum pH for this degradation reaction. In general, more active sites become available for photocatalytic processes when the catalyst dosage is increased, which can result in higher photocatalytic activity (Surakasi et al., 2022). The degradation efficiency of MB dye was increased with the increase in catalyst load up to 100 mg figure 12 (B) and maximum degradation observed at catalyst load 75 mg. Extra use of catalyst doze was un wanted according to atom economy. A lot of studies have seen into how the catalyst dose affects the photocatalytic activity of ZnO/SiO_2 NCs (Faisal, Jan, Shah, Shah, Khan, Akbar, Rizwan, Jan, Wajidullah, et al., 2021).

4.6.3. Effect of Initial Concentration of Methylene Blue (MB) Solution

The initial concentration of Methylene Blue (MB) solution was an important factor that could affect the photocatalytic degradation rate of MB that used ZnO NP, and ZnO/SiO_2 NCs. The effect of different MB dye concentration was studied by various concentrations (5, 15, 25, 35, and 45 ppm) by assigning catalyst load 75 mg, pH 6 and irradiation time 30 minutes the result plotted as follows in figure 12 (C) below. Generally, higher initial concentrations of MB result in slower degradation rates, as there are more MB molecules that need to be degraded, and the available active sites on the catalyst particles become saturated more quickly.

In general, the best initial MB concentration for photocatalytic processes involving ZnO/SiO_2 NCs may change based on the particular application and the kind of pollutant being eliminated. To achieve the best potential photocatalytic activity while preventing the detrimental consequences of excessive MB concentrations, the starting MB concentration must be carefully optimized.

4.6.4 Effect of Time in MB Dye Removal

The effect of removal time on the photodegradation efficiency of methylene blue was carried out by measuring the photodegradation efficiency at different periods of time using 75 mg of catalyst and 100 mL of 25 ppm dye solution with pH 6 under visible light at 30 ˚C. The results obtained appear in Figure 12 (D). The results revealed that the photocatalytic activity increases with an increase in the illumination time and reaches 100 % after 30 min illumination time. Such data reveals the relatively high activity of the prepared catalysts which enables the complete degradation of the methylene blue in such short illumination time, and the catalyst has active sites for carrying out the reaction.

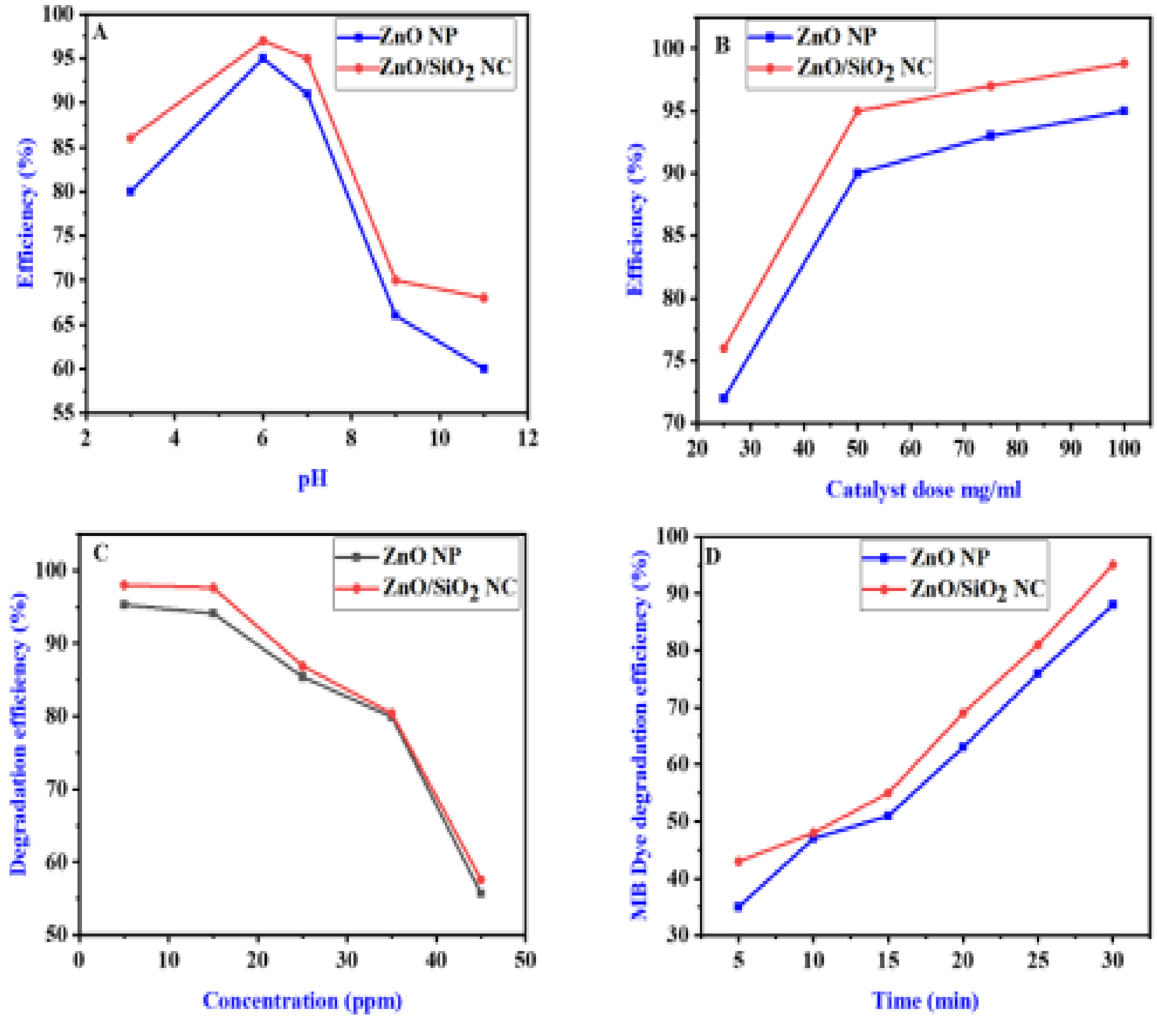

FIGURE 12: Optimization parameters of (A) pH, (B) Catalyst dosage, (C) Dye Concentration against degradation efficiency, and (D) time of ZnO NP, and ZnO/SiO_2 NC.

4.7. Kinetic Study of Synthesized ZnO NP and ZnO/SiO_2 NCs

Kinetic studies of ZnO NP, and ZnO/SiO_2 NCs have been conducted to understand the mechanism of photocatalytic degradation of various pollutants (Galedari et al., 2017). The photocatalytic activity of the synthesized ZnO NP, and ZnO/SiO_2 NC for the degradation of MB dye solution under sunlight (open) irradiation, and to compare the photocatalytic activity of each nanomaterial. The photodegradation of an aqueous solution of concentration of 100 ml of methylene blue (MB) solution 25 ppm by adding 75 mg of catalyst. By maintaining the open sunlight, and pH 6 at a time interval of 5 minutes for 30 minutes of light irradiation. The rate constant was found to increase with increasing catalyst dosage, indicating that the photocatalytic activity of ZnO NP, and ZnO/SiO_2 NCs is dependent on the amount of catalyst used (Galedari et al., 2017).

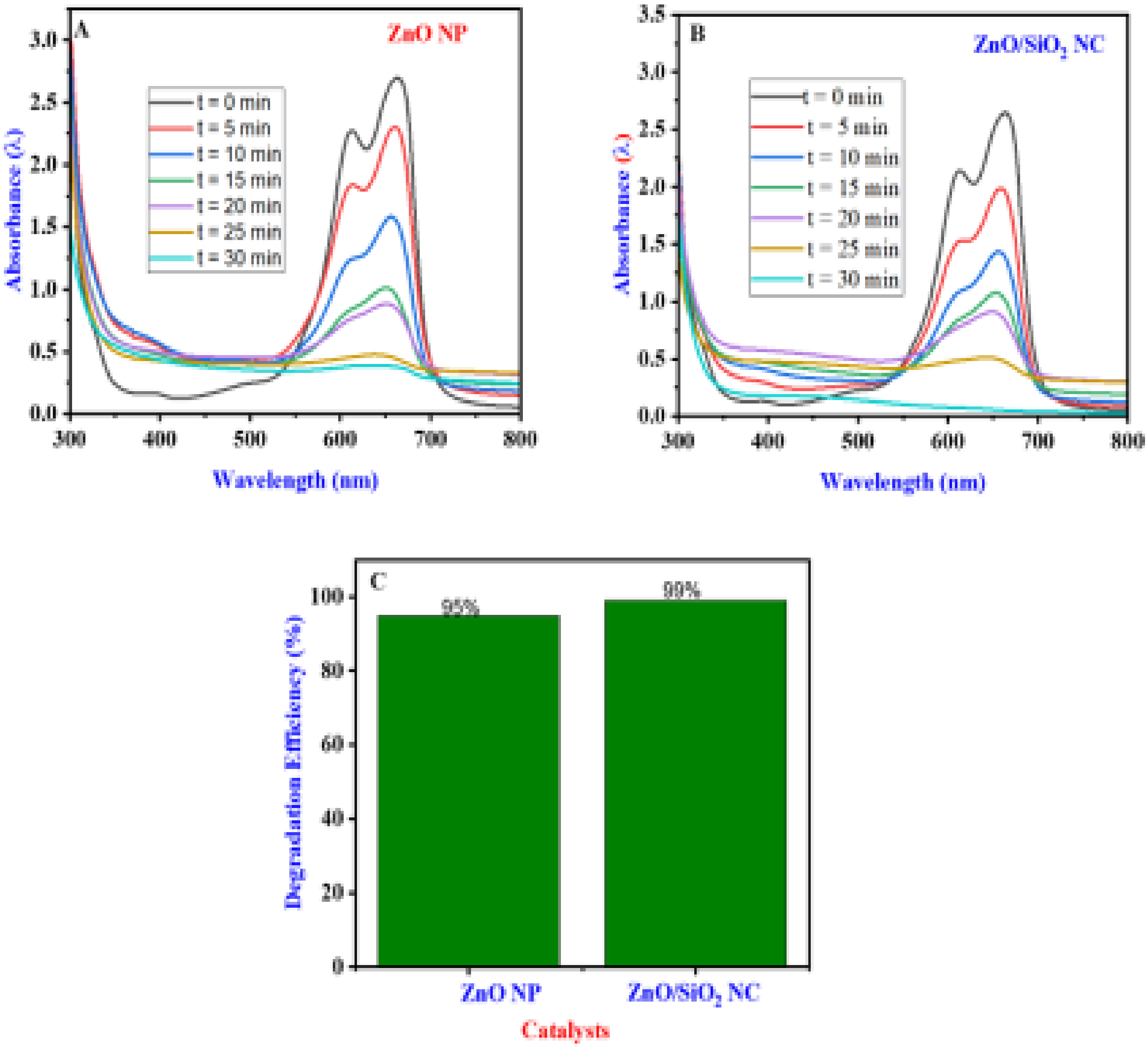

FIGURE 13: UV-Vis spectra of MB degradation by (A) ZnO NP, (B) ZnO/SiO_2 NC, and (C) Removal efficiency of synthesized nanomaterials.

The photo-degradation rate of methylene blue (MB) was calculated by the following

$$\text{Degradation}(\%)=\frac{A0-At}{A0}\ \text{x}\ 100 \quad\ldots\ldots\ldots\ldots\ldots\ldots\ldots\ldots\ldots\ldots\ldots\ldots\ldots\ldots 1$$

where A0 is the absorbance of initial MB; At is the absorbance of the solution after illumination at time t. According to the first-order kinetics reaction, rate constant k (min^{-1})

$$\ln\left(\frac{ct}{co}\right) = -kt \ldots\ldots\ldots\ldots\ldots\ldots\ldots\ldots\ldots\ldots\ldots\ldots\ldots\ldots\ldots\ldots\ldots\ldots 2$$

where Co and Ct are concentrations at the beginning and at a certain time t is the irradiation time. Adsorption kinetics investigations were carried out by agitating 25 ppm in 100 ml of

MB dye solution of known initial concentration with 75 mg of adsorbent prepared by ZnO/SiO_2 NCs (pH =6).

The photocatalytic activities of pure mixed ZnO and SiO_2 were tested in a conical flask under open sunlight irradiation. 75 mg of the photocatalysts were introduced at 25 ppm in 100 ml of an aqueous solution of methylene blue dye solution, pH = 6.

Overall, ZnO/SiO_2 NC kinetic studies indicate that depending on the particular pollutant and reaction conditions, either first-order or second-order kinetics govern the photocatalytic degradation of pollutants utilizing ZnO/SiO_2 NCs. The kinetics can offer insightful information about the photocatalytic process and be utilized to refine the process parameters for effective pollutant degradation (Alkaykh et al., 2020).

TABLE **7**: Different parameters of the pseudo-first-order and pseudo-second order kinetics

Catalyst	**Pseudo-first-order kinetics parameters**				**Pseudo-second-order kinetics parameters**			
	K1 (min^{-1})	R^2	Slope	Intercept	K2 (min^{-1})	R^2	Slope	Intercept
ZnO/SiO_2 NC	0.0047	0.94	0.0268	-0.0015	0.201	0.99	0.080	0.0318

The photocatalytic degradation of methylene blue checked by the pseudo-first and second order kinetic according to the Langmuir-Hinshel-wood model. Figure 14 A shows the nonlinear relationship b/n Ln (Ct / Co) and the reaction time, confirming the degradation of MB solution not fitted with pseudo first-order kinetics. The value of R^2 calculated from the pseudo-second-order model is more closely one; this indicates that the pseudo-second-order model fit as shown on figure 14 B. The high photocatalytic rate is obtained for ZnO/SiO_2 NC. It can be concluded that pseudo-second-order modal was the best fit for degradation of MB using ZnO/SiO_2 NC, the same result were obtained in the previous study (Hassan et al., 2022). Linear regression correlation coefficient (R^2) or high correlation coefficients indicate that experimental data exhibit a good compliance with pseudo-second order kinetic model. The compliance with the pseudo-second-order model suggested that chemical sorption involving valence forces through sharing or exchange of electrons b/n adsorbent and adsorbate might be significant (Kaykhaii et al., 2018) .

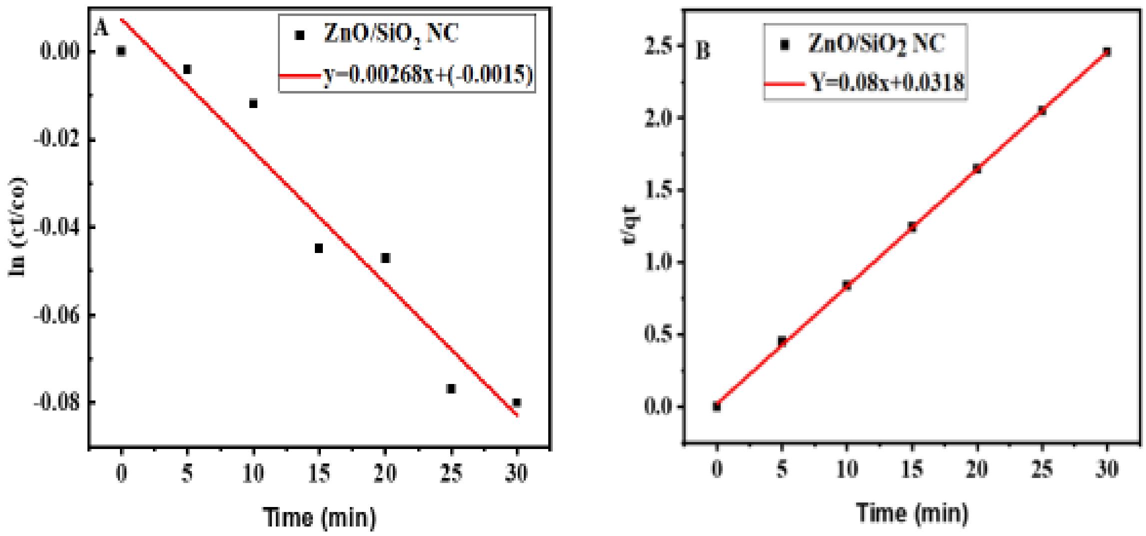

FIGURE 14: of (A) Pseudo-first-order and (B) Pseudo-second-order kinetic model for removal of methylene blue dye.

5. Conclusion and Recommendation

5.1 Conclusion

This study perfectly reports the merits of ZnO/SiO_2 NCs produced by green synthesis methods to investigate antibacterial and photocatalytic activities. The green synthesized nanocomposite of calculated average crystal size is 8.1737 nm which provides a small sufficient and large surface area. The antibacterial and photocatalytic activities were done by using ZnO/SiO_2 NCs. In the antibacterial study of ZnO/SiO_2 NCs, the inhibition zones measured were 15 mm to P. *Aeruginosa,* 20 mm to *E. coli*, 15 mm to *S. Aureus*, and 20 mm to *S. Pyogenesis*. *P. Aeruginosa* bacteria had resistance to ZnO NPs. The green synthesized ZnO/SiO_2 NC was sensitive to all tested bacterial strains in this study. In general, the green synthesized ZnO/SiO_2 NCs are a wonderful treatment provider for environmental pollution. The parameters such as the effect of pH of the dye solution, the catalyst load, dye concentration and kinetic properties of ZnO/SiO_2 NCs were similarly studied. The catalyst doze increased to 100 mg, as a result the photocatalytic degradation of MB dye was highly increased efficiency of removal. The high photocatalytic rate is obtained for ZnO/SiO_2 NC. It can be concluded that pseudo-second-order modal was the best fit for degradation of MB using ZnO/SiO_2 NC. Therefore, green synthesized ZnO/SiO_2 NC was effective in both antibacterial and photocatalytic activities.

5.2. Recommendation

1. To supply full information of ZnO/SiO_2 nanocomposites, the author of this thesis recommend that the chemical composition of the synthesized samples should be characterized by X-ray photoelectron spectroscopy. To investigate the particle size, more detailed morphology, and surface area of nanocomposite should be characterized by TEM and Brunauer-Emmett-Teller (BET) instruments respectively.

2. The spread of bacterial infectious diseases is now a day challenge of human health; so it is significant to control these bacterial diseases by using green synthesized ZnO/SiO_2 NC.

3. It is important to use green synthesized ZnO/SiO_2 NCs for effective photocatalytic activity on organic dye removal.

References

Ahmed, S., Annu, Chaudhry, S. A., & Ikram, S. (2017). A review on biogenic synthesis of ZnO nanoparticles using plant extracts and microbes: A prospect towards green chemistry. *Journal of Photochemistry and Photobiology B: Biology*, *166*, 272–284. https://doi.org/10.1016/j.jphotobiol.2016.12.011

Al-Tayyar, N. A., Youssef, A. M., & Al-Hindi, R. R. (2020). Antimicrobial packaging efficiency of ZnO-SiO2 nanocomposites infused into PVA/CS film for enhancing the shelf life of food products. *Food Packaging and Shelf Life*, *25*(January), 100523. https://doi.org/10.1016/j.fpsl.2020.100523

Alene, M., Abdelwuhab, M., Belay, A., & Yazie, T. S. (2020). Evaluation of Antidiabetic Activity of Ajuga integrifolia (Lamiaceae) Root Extract and Solvent Fractions in Mice. *Evidence-Based Complementary and Alternative Medicine*, *2020*. https://doi.org/10.1155/2020/6642588

Ali, J. A., Kolo, K., Mohammed Sajadi, S., Manshad, A. K., & Stephen, K. D. (2019). Green synthesis of ZnO/SiO2 nanocomposite from pomegranate seed extract: Coating by natural xanthan polymer and its characterisations. *Micro and Nano Letters*, *14*(6), 638–641. https://doi.org/10.1049/mnl.2018.5617

Alkaykh, S., Mbarek, A., & Ali-Shattle, E. E. (2020). Photocatalytic degradation of methylene blue dye in aqueous solution by MnTiO3 nanoparticles under sunlight irradiation. *Heliyon*, *6*(4), e03663. https://doi.org/10.1016/j.heliyon.2020.e03663

Alosaimi, E. H., Alsohaimi, I. H., Dahan, T. E., Chen, Q., Younes, A. A., El-Gammal, B., & Melhi, S. (2021). Photocatalytic Degradation of Methylene Blue and Antibacterial Activity of Mesoporous TiO2-SBA-15 Nanocomposite Based on Rice Husk. *Adsorption Science and Technology*, *2021*. https://doi.org/10.1155/2021/9290644

Balcha, A., Yadav, O. P., & Dey, T. (2016). Photocatalytic degradation of methylene blue dye by zinc oxide nanoparticles obtained from precipitation and sol-gel methods. *Environmental Science and Pollution Research*, *23*(24), 25485–25493. https://doi.org/10.1007/s11356-016-7750-6

Bandeira, M., Giovanela, M., Roesch-ely, M., Devine, D. M., & Crespo, S. (2020). Green synthesis of zinc oxide nanoparticles : A review of the synthesis methodology and mechanism of formation. *Sustainable Chemistry and Pharmacy*, *15*(January), 100223.

https://doi.org/10.1016/j.scp.2020.100223

Carrouel, F., Viennot, S., Ottolenghi, L., Gaillard, C., & Bourgeois, D. (2020). Nanoparticles as anti-microbial, anti-inflammatory, and remineralizing agents in oral care cosmetics: A review of the current situation. In *Nanomaterials* (Vol. 10, Issue 1). https://doi.org/10.3390/nano10010140

Durgude, S. A., Ram, S., Kumar, R., Singh, S. V., Singh, V., Durgude, A. G., Pramanick, B., Maitra, S., & Gaber, A. (2022). *Synthesis of Mesoporous Silica and Graphene-Based FeO and ZnO Nanocomposites for Nutritional Biofortification and Sustained the Productivity of Rice (Oryza sativa L .). 2022*.

Eletta, O. A. A., Mustapha, S. I., Ajayi, O. A., & Ahmed, A. T. (2018). Optimization of dye removal from textile wastewater using activated carbon from sawdust. *Nigerian Journal of Technological Development*, *15*(1), 26. https://doi.org/10.4314/njtd.v15i1.5

Fabiana Meijon Fadul. (2019).

Faisal, S., Jan, H., Shah, S. A., Shah, S., Khan, A., Akbar, M. T., Rizwan, M., Jan, F., Wajidullah, Akhtar, N., Khattak, A., & Syed, S. (2021). Green Synthesis of Zinc Oxide (ZnO) Nanoparticles Using Aqueous Fruit Extracts of Myristica fragrans: Their Characterizations and Biological and Environmental Applications. *ACS Omega*, *6*(14), 9709–9722. https://doi.org/10.1021/acsomega.1c00310

Farrukh, A. (2016). Antibacterial and Antifungal Activities of Zinc-Silicon Oxides Nanocomposite. *Lettters in Health & Biological Sciences*, *1*(1), 1–5. https://doi.org/10.15436/2475-6245.16.003

Fatimah, I., Fadillah, G., Sahroni, I., & Kamari, A. (2021). Nanoflower-like composites of ZnO / SiO 2 synthesized using bamboo leaves ash as reusable photocatalyst. *Arabian Journal of Chemistry*, *14*(3), 102973. https://doi.org/10.1016/j.arabjc.2020.102973

Galedari, N. A., & Rahmani, M. (2016). Preparation , characterization , and application of ZnO @ SiO 2 core – shell structured catalyst for photocatalytic degradation of phenol. *Environmental Science and Pollution Research*. https://doi.org/10.1007/s11356-016-7888-2

Galedari, N. A., Rahmani, M., & Tasbihi, M. (2017). Preparation, characterization, and application of ZnO@SiO2 core–shell structured catalyst for photocatalytic degradation of phenol. *Environmental Science and Pollution Research*, *24*(14), 12655–12663.

https://doi.org/10.1007/s11356-016-7888-2

Hassan, Y. M., Guan, B. H., Chuan, L. K., Hamza, M. F., Khandaker, M. U., Sikiru, S., Adam, A. A., Abdul Sani, S. F., Abdulkadir, B. A., & Ayub, S. (2022). The influence of ZnO/SiO2 nanocomposite concentration on rheology, interfacial tension, and wettability for enhanced oil recovery. *Chemical Engineering Research and Design*, *179*, 452–461. https://doi.org/10.1016/j.cherd.2022.01.033

Jamdagni, P., Khatri, P., & Rana, J. S. (2016). Green synthesis of zinc oxide nanoparticles using flower extract of Nyctanthes arbor-tristis and their antifungal activity. *Journal of King Saud University - Science*. https://doi.org/10.1016/j.jksus.2016.10.002

Javan, S., Djahaniani, H., Nabati, F., & Hekmati, M. (2020). *Heliyon Characterization and the evaluation of antimicrobial activities of silver nanoparticles biosynthesized from Carya illinoinensis leaf extract*. *6*(March).

Jayachandran, A., T.R., A., & Nair, A. S. (2021). Green synthesis and characterization of zinc oxide nanoparticles using Cayratia pedata leaf extract. *Biochemistry and Biophysics Reports*, *26*, 100995. https://doi.org/10.1016/j.bbrep.2021.100995

Justine, M., Joy Prabu, H., Johnson, I., Magimai Antoni Raj, D., John Sundaram, S., & Kaviyarasu, K. (2019). Synthesis and characterizations studies of ZnO and ZnO-SiO2nanocomposite for biodiesel applications. *Materials Today: Proceedings*, *36*(xxxx), 440–446. https://doi.org/10.1016/j.matpr.2020.05.034

Kaul, S., Gulati, N., Verma, D., Mukherjee, S., & Nagaich, U. (2018). Role of Nanotechnology in Cosmeceuticals: A Review of Recent Advances. *Journal of Pharmaceutics*, *2018*, 1–19. https://doi.org/10.1155/2018/3420204

Kaur, H. (2018). *Chemical investigation of medicinal plant Ajuga bracteosa Chemical investigation of medicinal plant Ajuga bracteosa*. *October*.

Kaykhaii, M., Sasani, M., & Marghzari, S. (2018). Removal of Dyes from the Environment by Adsorption Process. *Chemical and Materials Engineering*, *6*(2), 31–35. https://doi.org/10.13189/cme.2018.060201

Kokabi, M., Ebrahimi, S. N., & Zarei, M. (2017). *Green synthesis of zinc oxide nanoparticles using Seaweed aqueous extract and evaluation of antibacterial and ecotoxicological activity*. *June 2020*. https://doi.org/10.29252/jpg.8.27.61

Kumud, M., & Sanju, N. (2018). Nanotechnology Driven Cosmetic Products: Commercial and Regulatory Milestones. *Applied Clinical Research, Clinical Trials and Regulatory Affairs*, *5*(2), 112–121. https://doi.org/10.2174/2213476x05666180530093111

Liu, Y., & Chen, L. (2022). *SiO2 and ZnO Hybrid Nano llers Modi ed Natural Rubber Latex : Excellent Tensile Properties and Antibacterial Properties*.

Maijan, P., Amornpitoksuk, P., & Chantarak, S. (2020). Synthesis and characterization of poly(vinyl alcohol-g-acrylamide)/SiO2@ZnO photocatalytic hydrogel composite for removal and degradation of methylene blue. *Polymer*, *203*, 122771. https://doi.org/10.1016/j.polymer.2020.122771

Mansoori, G. A. (2017). *An Introduction to Nanoscience and Nanotechnology*. https://doi.org/10.1007/978-3-319-46835-8

Mao, H., Zhang, B., Nie, Y., Tang, X., Yang, S., & Zhou, S. (2021). Enhanced antibacterial activity of V-doped ZnO@SiO2 composites. *Applied Surface Science*, *546*(January), 149127. https://doi.org/10.1016/j.apsusc.2021.149127

Mohamed, R. M., Mkhalid, I. A., Baeissa, E. S., & Al-Rayyani, M. A. (2012). Photocatalytic degradation of methylene blue by Fe/ZnO/SiO 2 nanoparticles under visiblelight. *Journal of Nanotechnology*, *2012*. https://doi.org/10.1155/2012/329082

Muhammad, G., Mehmood, S., Zafar, R., Manj, A., Mahmood, S., Hassan, N., & Ali, M. A. (2021). *Effect Of ZnO Nanoparticles on the Physical , Chemical and Nutritional Quality of Tomato Plant (Solanum Lycopersicum)*. 31602–31608. https://doi.org/10.26717/BJSTR.2021.39.006351

Narendra Kumar, H. K., Chandra Mohana, N., Nuthan, B. R., Ramesha, K. P., Rakshith, D., Geetha, N., & Satish, S. (2019). Phyto-mediated synthesis of zinc oxide nanoparticles using aqueous plant extract of Ocimum americanum and evaluation of its bioactivity. *SN Applied Sciences*, *1*(6), 1–9. https://doi.org/10.1007/s42452-019-0671-5

Naseer, M., Aslam, U., Khalid, B., & Chen, B. (2020). Green route to synthesize Zinc Oxide Nanoparticles using leaf extracts of Cassia fistula and Melia azadarach and their antibacterial potential. *Scientific Reports*, 1–10. https://doi.org/10.1038/s41598-020-65949-3

Nazarkovsky, M., Czech, B., Żmudka, A., Bogatyrov, V. M., Artiushenko, O., Zaitsev, V., Saint-Pierre, T. D., Rocha, R. C., Kai, J., Xing, Y., Gonçalves, W. D. G., Veiga, A. G., Rocco, M. L. M., Safeer, S. H., Galaburda, M. V., Carozo, V., Aucélio, R. Q., Caraballo-Vivas, R. J., Oranska, O. I., & Dupont, J. (2021). Structural, optical and catalytic properties of ZnO-SiO2 colored powders with the visible light-driven activity. *Journal of Photochemistry and Photobiology A: Chemistry*, *421*(February). https://doi.org/10.1016/j.jphotochem.2021.113532

Nozari, B., Montazer, M., & Mahmoudi Rad, M. (2021). Stable ZnO/SiO2 nano coating on polyester for anti-bacterial, self-cleaning and flame retardant applications. *Materials Chemistry and Physics*, *267*(April), 124674. https://doi.org/10.1016/j.matchemphys.2021.124674

Panigrahi, S., Bera, A., & Basak, D. (2011). Ordered dispersion of ZnO quantum dots in SiO2 matrix and its strong emission properties. *Journal of Colloid and Interface Science*, *353*(1), 30–38. https://doi.org/10.1016/j.jcis.2010.09.055

Pelgrift, R. Y., & Friedman, A. J. (2013). Nanotechnology as a therapeutic tool to combat microbial resistance. *Advanced Drug Delivery Reviews*. https://doi.org/10.1016/j.addr.2013.07.011

Purohit, M. C., Kandwal, A., Khajuria, A. K., Singh, M., & Rawat, R. (2020). *ANTIMICROBIAL ACTIVITY OF AJUGA PARVIFLORA LEAF EXTRACT*. *20*, 1627–1630.

Rahimzadeh, C. Y., Barzinjy, A. A., Salih, A., & Id, M. (2022). *Green synthesis of SiO 2 nanoparticles from Rhus coriaria L . extract : Comparison with chemically synthesized SiO 2 nanoparticles*. *August*. https://doi.org/10.1371/journal.pone.0268184

Ren, L., Zhao, G., Pan, L., Chen, B., Chen, Y., Zhang, Q., Xiao, X., & Xu, W. (2021). *E ffi cient Removal of Dye from Wastewater without Selectivity Using Activated Carbon-Juncus ef f usus Porous Fibril Composites*. https://doi.org/10.1021/acsami.0c22104

Rl, M., Kv, U., & Naik, D. (2019). *Synthesis and characterization of ZnO nanoparticles : A review*. *8*(3), 1095–1101.

Ruhul, M., & Bhuiyan, A. (2021). *A Brief Review of the Synthesis of ZnO Nanoparticles for Biomedical A Brief Review on the Synthesis of Zno Nanoparticles for Biomedical Applications*. *September*. https://doi.org/10.22068/ijmse.1995

Safavinia, L., Akhgar, M. R., Tahamipour, B., & Ahmadi, S. A. (2021). *Green Synthesis of Highly Dispersed Zinc Oxide Nanoparticles Supported on Silica Gel Matrix by Daphne oleoides Extract and their Antibacterial Activity*. *19*(January).

https://doi.org/10.30498/IJB.2021.2598

Safawo, T., Sandeep, B. V, Pola, S., & Tadesse, A. (2018). OpenNano Synthesis and characterization of zinc oxide nanoparticles using tuber extract of anchote (Coccinia abyssinica (Lam .) Cong .) for antimicrobial and antioxidant activity assessment. *OpenNano*, *3*(May), 56–63. https://doi.org/10.1016/j.onano.2018.08.001

Sampson, G. R. (2019). *G.R. Sampson: library catalogue*.

Saravanan, S. (2020). *Synthesis of SiO2 Nanoparticles by Sol-Gel Method and Their Optical and Synthesis of SiO 2 Nanoparticles by Sol-Gel Method and Their Optical and Structural Properties*. *June 2021*.

Sekhar, D. C., Diwakar, B. S., & Madhavi, N. (2019). Synthesis, characterization and anti-bacterial screening of complex nanocomposite structures of SiO2@ZnO@Fe3O4 and SnO2@ZnO@Fe3O4. *Nano-Structures and Nano-Objects*, *19*. https://doi.org/10.1016/j.nanoso.2019.100374

Senthil Kumar, P., Janet Joshiba, G., Femina, C. C., Varshini, P., Priyadharshini, S., Arun Karthick, M. S., & Jothirani, R. (2019). A critical review on recent developments in the low-cost adsorption of dyes from wastewater. *Desalination and Water Treatment*, *172*, 395–416. https://doi.org/10.5004/dwt.2019.24613

Shafiei, N., Nasrollahzadeh, M., & Iravani, S. (2021). Comments on Inorganic Chemistry A Journal of Critical Discussion of the Current Literature Green Synthesis of Silica and Silicon Nanoparticles and Their Biomedical and Catalytic Applications Green Synthesis of Silica and Silicon Nanoparticles and. *Comments on Inorganic Chemistry*, *00*(00), 1–56. https://doi.org/10.1080/02603594.2021.1904912

Sharma, A., Pallavi, Sanjay, & Dahiya, S. (2012). Synthesis and characterization of calcinated ZnO nanoparticles. *AES-ATEMA International Conference Series - Advances and Trends in Engineering Materials and Their Applications*, *5*(6), 69–74.

Sharma, P. K., Dutta, R. K., Kumar, M., Singh, P. K., & Pandey, A. C. (2009). Luminescence studies and formation mechanism of symmetrically dispersed ZnO quantum dots embedded in SiO2 matrix. *Journal of Luminescence*, *129*(6), 605–610. https://doi.org/10.1016/j.jlumin.2009.01.004

Sharma, P., Kherb, J., Prakash, J., & Kaushal, R. (2021). A novel and facile green synthesis of - SiO 2 nanoparticles for removal of toxic water pollutants. *Applied Nanoscience*, *0123456789*. https://doi.org/10.1007/s13204-021-01898-1

Spoiala, A., Albu, M. G., Ficai, A., Andronescu, E., Voicu, G., & Ungureanu, C. (2014). The SiO2/ZnO composite materials for cosmetic creams. *Digest Journal of Nanomaterials and Biostructures*, *9*(4), 1729–1737.

Sportelli, M. C., Gaudiuso, C., Volpe, A., Izzi, M., Picca, R. A., Ancona, A., & Cioffi, N. (2022). *Biogenic Synthesis of ZnO Nanoparticles and Their Application as Bioactive Agents : A Critical Overview*. 423–441.

Surakasi, R., Alimuddin, Rao, Y. S., Sanuj, A. K., Patil, P. P., Jayaganthan, A., & Hechhu, R. (2022). Methylene Blue Dye Photodegradation during Synthesis and Characterization of WO3Nanoparticles. *Adsorption Science and Technology*, *2022*. https://doi.org/10.1155/2022/2882048

Yang, S., Nie, Y., Zhang, B., Tang, X., & Mao, H. (2020). Construction of Er-doped ZnO/SiO2 composites with enhanced antimicrobial properties and analysis of antibacterial mechanism. *Ceramics International*, *46*(13), 20932–20942. https://doi.org/10.1016/j.ceramint.2020.05.149

Zharov, V. P., Kim, J., Curiel, D. T., & Everts, M. (2005). *Self-assembling nanoclusters in living systems : application for integrated photothermal nanodiagnostics and nanotherapy*. *1*, 326–345. https://doi.org/10.1016/j.nano.2005.10.006